Surfaces and Interfaces

The role of interfacial oxygen in the nucleation and stability of Ni Nanoclusters at MgO ultrathin films: Insights from STM and first-principles DFT calculations

--Manuscript Draft--

Manuscript Number:	SURFIN-D-26-05175R1
Article Type:	Research Paper
Keywords:	Ni Nanoclusters; STM; DFT; Model Heterogeneous Catalysts; surface science; Sintering Prevention
Corresponding Author:	Sergio Tosoni, PhD University of Milan-Bicocca Milano, ITALY
First Author:	Mirali Jahangirzadeh Varjovi
Order of Authors:	Mirali Jahangirzadeh Varjovi
	Anshika Singh
	Elina Mkrtchian
	Mario Rocca
	Luca Vattuone
	Letizia Savio
	Sergio Tosoni, PhD
Abstract:	The interaction between metal nanoclusters and oxide surfaces plays a crucial role in determining the properties of materials for catalytic and electronic applications. Here we present a combined experimental scanning tunnelling microscopy and first-principles calculations study of the nucleation and spatial distribution of Ni nanoclusters grown by deposition of Ni atoms on MgO monolayer films supported on Ag(100) at temperature between 100 K and 300 K. Clusters compatible in size with the magic number 13, 55 and 147 compact icosahedral structures are metallic, but partially oxidized in the contact area with the MgO film. They also show a markedly different spatial distribution with deposition temperature: up to 250 K they sit mainly on flat MgO terraces, while at 300 K they accumulate almost exclusively at the steps. Both effects are caused by the unavoidable presence of oxygen atoms at the MgO/Ag interface, whose concentration decreases dramatically just below room temperature.
Response to Reviewers:	

Powered by Editorial Manager® and ProduXion Manager® from Aries Systems Corporation

Revised Manuscript Unmarked
Click here to view linked References

The role of interfacial oxygen in the nucleation and stability of Ni nanoclusters at MgO ultrathin films: Insights from STM and first-principles DFT calculations

Mirali Jahangirzadeh Varjovi[1*], Anshika Singh[2*], Elina Mkrtchian[3,4], Mario Rocca[2,3], Luca Vattuone[2,3], Letizia Savio[3#], Sergio Tosoni[1#]

[1]*Department of Materials Science, University of Milano-Bicocca, 20125 Milano, Italy*

[2]*Department of Physics, University of Genova, via Dodecaneso 33, 16146 Genova, Italy*

[3]*IMEM-CNR, UOS Genova, via Dodecaneso 33, 16146 Genova, Italy*

[4]*Department of Mathematical, Physical and Computer Sciences, University of Parma, 43124 Parma, Italy*

* *These authors contributed equally*

\# *Corresponding authors: sergio.tosoni@unimib.it, letizia.savio@cnr.it*

Abstract

The interaction between metal nanoclusters and oxide surfaces plays a crucial role in determining the properties of materials for catalytic and electronic applications. Here we present a combined experimental scanning tunnelling microscopy and first-principles calculations study of the nucleation and spatial distribution of Ni nanoclusters grown by deposition of Ni atoms on MgO monolayer films supported on Ag(100) at temperature between 100 K and 300 K. Clusters compatible in size with the magic number 13, 55 and 147 compact icosahedral structures are metallic, but partially oxidized in the contact area with the MgO film. They also show a markedly different spatial distribution with deposition temperature: up to 250 K they sit mainly on flat MgO terraces, while at 300 K they accumulate almost exclusively at the steps. Both effects are caused by the unavoidable presence of oxygen atoms at the MgO/Ag interface, whose concentration decreases dramatically just below room temperature.

1. Introduction

Catalysis plays a fundamental role in the production of goods and energy in contemporary society.[1] Its relevance is steadily increasing as the paradigm shifts toward circular pathways and the exploitation of renewable energy sources.[2-4] In particular, most employed catalytic systems fall under the definition of heterogeneous catalysts, in which the active species is a (more or less) small metal particle anchored on a solid support.[5-7] Reducing the size of a supported metal catalyst to the nanoscale is beneficial for saving precious raw materials, maximizing the mass/activity ratio, and increasing the catalyst activity.[8-9] E.g., a recent Density Functional Theory (DFT) and microkinetic study demonstrated that nickel nanoparticles with 1.7 nm size are expected to have the highest catalytic performance for CO_2 methanation.[10]

Catalytic reactions often occur at relatively high temperatures, where sintering may take place. The ability to control the size and the properties of supported nanoparticles is thus essential for further optimization of the heterogeneous catalyst. In this respect, the interaction with the

support plays a significant role. On the one hand, it ultimately controls the stability of the active particles and their tendency to undergo sintering and thermal deactivation.[11-17] Indeed, it was shown that Ag clusters stop sintering at a diameter of 6 nm on MgO but only of ~3 nm on Ceria.[18] On the other hand, chemical and structural changes induced by the support on the metal particles can deeply affect their chemical properties and reactivity.

It is thus interesting to complement applied studies in catalysis, where the activity and turnover frequency of a given system are the main figures of merit, with more basic works, aimed at the thorough characterization of the structural properties of supported metal nanoparticles and their interaction with the support. This eventually justified the effort to grow insulating oxides as ultrathin films on metal surfaces: such systems allow the study of wide-gap oxides (often used as supports in catalytic processes) using electron-based techniques. In particular, high-resolution scanning tunnelling microscopy can be employed, exploiting the electron tunnelling effect enabled by the extreme thinness of the oxide film.[19-20] However, ultra-thin oxide films exhibit peculiar chemical and physical properties, distinguishing them from their bulk counterparts.[20-23] In particular, magnesium oxide (MgO) has attracted remarkable attention due to its good lattice match with metal supports such as silver (Ag) and molybdenum (Mo), enabling the epitaxial growth of ordered films.[24] Additionally, it was reported that the electron transfer via tunnelling through the MgO film induces the formation of negatively charged, highly reactive sub-nanometric Au particles.[25-26]

Despite the relative structural simplicity of the interface between rock salt MgO and the Ag(100) cubic lattice, numerous papers have shown that the preparation conditions remarkably influence the morphology of the films. For instance, several reports describe the formation of MgO bilayers epitaxially grown on Ag(001),[27] while some of us reported and characterized the formation of extended monolayers.[28] Notably, given the non-negligible oxophilicity of silver,[29] a certain concentration of oxygen is unavoidably trapped at the MgO/Ag interface during the growth process, with relevant impact on the work function of the system and on interfacial charge transfer phenomena. Its optimal concentration was estimated as 25% recurring to ab initio thermodynamics, in good agreement with the value of 30% estimated experimentally at 200 K.[30] However, regions with different loading of interfacial oxygen (O_{int}) can form during the growth process underneath any given MgO island.[31] Such interfacial oxygen can diffuse to the external layer leading to a complete oxidation of the smallest nickel aggregates (in the range of 4-6 atoms) under ultra-high vacuum conditions.[32]

Larger Ni aggregates on MgO/Ag(100) are, on the contrary, mainly metallic.[33] DFT calculations recently performed by some of us showed that such clusters are slightly negatively charged in the absence of O_{int} whereas they assume a slightly positive charge in its presence. This positive charge may increase significantly due to a thermodynamically favourable reverse oxygen spillover phenomenon leading O atoms to diffuse from the MgO/Ag interface through the MgO film and bind to the Ni clusters.[34] This is an important observation, since the oxidation state of Ni particles, often observed for real catalytic systems under operando conditions, strongly influences their chemical reactivity.[35-43]

In the present paper, we shall demonstrate by comparing experimental data with DFT calculations that these Ni nanoclusters (NCs) indeed have an oxidized root and that the

interfacial oxygen concentration determines their spatial distribution at terrace and step sites of the MgO film. These findings are of high importance for the rational design of heterogeneous catalysts, where the strength of the adhesion to the support dictates the activity of the supported particles, and their resistance toward sintering and thermal deactivation.[44]

2. Experimental and theoretical section

Experiments were carried out in an ultrahigh vacuum system hosting a LT-STM (Createc) and connected to a preparation chamber equipped with a Knudsen cell and an O_2 doser for reactive Mg evaporation, a quartz microbalance (QMB) for Mg flux measurements, an e-beam evaporator (Focus EFM 3) mounting a high-purity (99.99%) Ni rod, and with additional facilities for sample cleaning and residual gas analysis.

The Ag(100) substrate is a single crystal cut within 0.1° off the high symmetry plane. Before each experiment, the sample is carefully cleaned by sputtering with Ne^+ ions followed by annealing to a temperature T= 850 K for 5 minutes. Surface cleanliness and order were checked by STM. Monolayer MgO films were grown by reactive deposition at T= 773 K, followed by post-annealing in O_2 atmosphere and slow cooling to T< 450 K.[28] Mg was evaporated from a crucible at T_{ev}=593 K, providing an Mg flux of ∼1 Å/min., in an O_2 pressure $P_{O2}= 1 \times 10^{-6}$ mbar; however, since the oxygen was introduced in the preparation chamber through a doser placed at ∼2 cm from the Ag(100) surface, an effective pressure at least five times higher is expected.[45] Ni was deposited on the MgO/Ag(100) sample at 100 K≤T≤300 K in a background pressure better than 2×10^{-9} mbar. The Ni flux could not be measured during evaporation, so the total Ni coverage is evaluated a posteriori from analysis of STM images, accounting for the different sizes and shapes of the clusters at different deposition temperatures. Samples are cooled to T< 150 K and inserted into the STM immediately after preparation. STM images were recorded at liquid nitrogen temperature with a Pt/Ir tip cut in air under strain and then reshaped by controlled crashes into the surface, so that tunnelling effectively occurs through an Ag tip. The images were acquired in constant current mode, with typical tunnelling currents of ∼ 0.2 nA and bias voltage applied to the sample, −4.0 V≤ V ≤ +4.0 V. The lateral size of the images and the orientation of the surface are determined from atomically resolved measurements of the clean Ag(100) surface (as the one reported in Figure 1f); similarly, heights are calibrated against monatomic Ag steps. STM analysis was performed with the help of WSxM software.[46]

In this study, all first-principles calculations were performed within the framework of spin-polarized DFT [23-24, 47-48] as implemented in the Vienna Ab initio Simulation Package (VASP).[25-27, 49-53] The exchange-correlation potential was parameterized using the Perdew–Burke–Ernzerhof (PBE) [54] functional within the generalized gradient approximation (GGA). The projector-augmented wave (PAW) [55] method was employed to describe the pseudopotentials for O, Mg, Ni, and Ag. A kinetic energy cutoff of $\frac{\hbar^2|k+G|^2}{2m} = 520\ eV$ was employed for the plane-wave basis set, and a vacuum space of ∼20 Å was inserted in the non-periodic direction for all calculations involving clusters on different supports to prevent artificial interactions between neighbouring images. Brillouin zone (BZ) sampling for the relaxation of the MgO(100) monolayer and Ag(100) slab was performed using a Γ-centred

8 × 8 × 1 uniform k-point mesh.[56] For the optimization of NCs on various supports, VASP-Γ was employed with a 1×1×1 k-point grid, suitable for the large supercell sizes. Bader charge analysis was employed to obtain the net charge transfer between the clusters and the supports.[57] During total energy calculations, the electronic relaxation converged to a threshold of 10^{-5} eV between consecutive steps. The optimization of ionic positions and lattice constants was performed until the maximum force on each atom was below 0.01 eV/Å. Furthermore, long-range dispersion effects were considered using the D3 method from Grimme, which includes the Becke-Johnson damping function.[58-59] The magnetic configuration for all calculations was initialized consistently, with a singlet state for Mg, O, and Ag, and a triplet state for Ni, while allowing the configuration to evolve during the self-consistent field iterations. The adsorption energy of the nanoclusters (E_{ads}) can be computed via the following formula

$$E_{ads} = E(Ni_X /Support) – E(Ni_X) – E(Support) \quad (1)$$

where $E(Ni_X /Support)$ represents the total energy of the examined systems, $E(Ni_X)$ and E(Support) denote the total energies of the gas-phase NCs and the support, respectively, and x indicates the number of Ni atoms within the cluster (x=13, 55, 147).

3. Nucleation and migration of Ni Nanoclusters

Figure 1a)-d) shows STM images of Ni NCs grown on monolayer MgO/Ag(100) at four different temperatures: a) 100 K, b) 200 K, c) 250 K and d) 300 K. The protocol followed for the growth of the MgO monolayer is the one reported in ref.[28] leading to extended MgO islands limited only by the size of the Ag terrace underneath. Ni atoms are eventually evaporated by e-beam evaporation. After deposition, they aggregate forming Ni clusters. At 200 K, one-third of the Ni coverage consists of small Ni_xO_y clusters ($4 \leq x \leq 6$) while the rest aggregates into larger, metallic clusters.[33] At 300 K only the larger clusters form. Their apparent average diameter increases thereby from 10-12 Å at 100 K to 17-20 Å at 300 K. A qualitatively similar increase in the Ni/MgO contact area (while the cluster height is conversely reduced) was also noticed by means of Ab-Initio Molecular Dynamics simulations, comparing structures simulated at 0 K and 200 K.[34] Incidentally, dark spots are visible in Figs. 1a. An ultimate assignment on their nature cannot be provided, but we report that changes in contrast within MgO islands were previously attributed to non-uniform distribution of interfacial oxygen, affecting the local density of states of the MgO film.[31]”

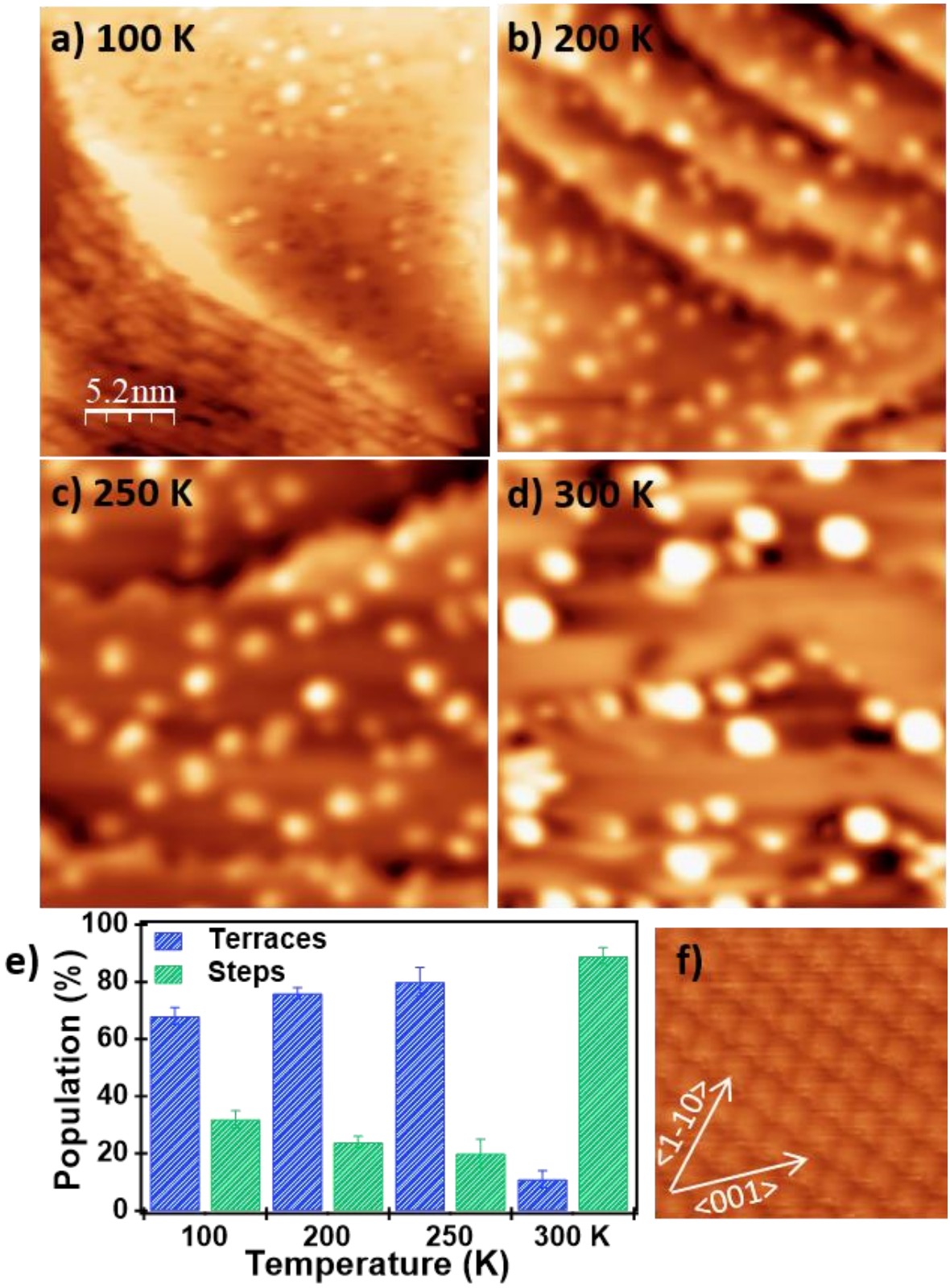


Figure 1. STM images of Ni NCs deposited at different temperatures on monolayer MgO/Ag(100). a) T=100 K, b) T=200 K, c) T=250 K, and d) T=300 K. For all images, size: 26 × 26 nm2; V =+1.0 V. e) Population of clusters at steps and terraces as a function of temperature. The percentages reported in the histogram and in the text are averages over a minimum of several STM images of size (26 × 26) nm^2 (10 images at 100 K, 13 images at 200

K, 5 images at 250 K and 11 images at 300 K). The standard error is reported. f) Atomically resolved image of the clean Ag(100) substrate, from which the high symmetry directions (marked by arrows) and the calibration parameters are deduced.

As evident at a first glance from Fig.1a)-d) and from the histogram of Fig. 1e), the distribution of Ni nanoclusters at MgO steps or terrace sites strongly depends on the deposition temperature: for T≤250 K, they are found mainly at terraces, while at 300 K, they decorate the steps. Indeed, the relative population of NCs at step sites is between 20 and 30% for T≤250 K but it jumps to (89±3) % at 300 K (see Table S1 in Supporting Material).

Formation of metal nanoparticles of larger diameter and the preferential population of clusters at steps with increasing temperature have also been reported for other systems, such as Cu atoms deposited on CeO1.95(111) and Au clusters on NaCl(001).[60-61] This behaviour can be rationalized by considering that, at low T, diffusion is slow and the metal atoms have a high probability of meeting another atom/cluster and aggregating before reaching a step. Although diffusion certainly also plays a role in the present case, the trend in relative population does not show any preferential nucleation at steps below 300 K, even though nanometric clusters grow also at lower temperature. The overviews in Figure a)-c) may appear different, but this is mainly due to the different step density of the imaged MgO areas since statistical analysis over several images (Figure 1e) indicates a similar population of Ni NCs at steps for T≤250 K. Vice versa, the outcome at 300 K suggests the activation of a different mechanism. As it will be discussed in the following, our findings envisage that the presence of interfacial oxygen between MgO and Ag could enhance the clusters stability on terraces. The limited thermal stability of O_{int}, though, may explain the preferential growth at steps at 300 K. We also remark that alternative explanations as the presence of F-centres or OH acting as nucleation centres at the terraces at low temperature can be excluded. On the one hand, oxygen vacancies are unlikely in presence of O_{int}; on the other hand, the presence of OH is ruled out by vibrational spectroscopy analysis performed during CO exposure on Ni NC/MgO/Ag(100) [33].

To gain more insight into this phenomenon, we performed DFT modelling of particles of comparable size to those observed in the STM measurements. First, we note that the measured cluster diameter should be corrected for convolution with the STM tip, so that a size in the range of 5 nm to 15 nm can be inferred. Given the highly complex polymorphism and the actual composition of supported metal clusters within the observed size range, we decided to focus on specific clusters exhibiting high stability in the gas phase. Therefore, we chose the icosahedral Ni_{13}, Ni_{55} and Ni_{147} clusters, corresponding to the "magic numbers" for which the nanoparticles exhibit complete outer atomic shells and compact structures.[62] It must be stated, however, that other geometries could as well be possible, and an exhaustive study of the polymorphism in supported particles is beyond the scope of the present work.

As shown in Fig. S1 of the Supporting Material, they are all characterized by triangular closed packed nanofacets; in the gas phase their diameter spans from 4.67 Å (Ni_{13}), to 9.24 Å (Ni_{55}), and to 13.93 Å (Ni_{147}) (see Table 1).

The adsorption of these clusters was simulated on the various MgO supports on Ag(100) schematized in Fig. S2: a continuous MgO monolayer (ML_c, panel a), a finite monolayer

MgO island (ML_i, panel b), a continuous MgO bilayer (BL_c, panel c), and a stepped MgO BL (BL_s, panel d).

The results of the simulations are reported in Table 1. The side views of the corresponding relaxed structures are shown in Fig. 2. First, one can notice that the icosahedral clusters maintain a quasi-spherical geometrical arrangement on all MgO supports: their height with respect to the surface (measured as the difference in the z coordinate between the apical Ni atom of the cluster and the basal MgO plane) and their diameter display very similar values (Table 1, col. III and IV). On ML_i, the clusters sit at the edge of the MgO island, in contact with the bare Ag. In this case, Ni55 and Ni147 clusters retain their quasi-spherical shape, while the Ni13 ones wet the bare metal. We remark that, in general, the calculated physical heights exceed the values previously reported in ref. [33]; however, the latter ones correspond to the apparent height measured by STM, so that a direct comparison is misleading. The clusters' magnetization (Table 1, col. V) does not undergo drastic changes relative to the gas-phase, with a general small increase (Ni_{13}) or small decrease (Ni_{55} and Ni_{147}). Ni_{13} maintains an almost neutral charge state upon adsorption on the various MgO supports featured in Figure 2. At the same time, Ni_{55} and Ni_{147} acquire a sizable negative charge, with little difference on MLs or BLs (col. VI). Interestingly, the interfacial dipole (col. VII) does not correlate with such a charge transfer: if negative charge is injected into a metal cluster adsorbed on the surface, a positive dipole moment would be expected; however, neither its sign nor its intensity shows a regular trend. This could be explained by an internal compensation effect among the dipole moment generated at the MgO/Ag interface, the contribution of charge transfer to the adsorbed Ni cluster, and charge redistribution phenomena within the metal particle.

Table 1. Ni_X (X=13, 55, 147) adsorbed on a continuous MgO ML/Ag (ML_c), an MgO ML island on Ag (ML_i), a continuous MgO BL/Ag (BL_c), and a stepped MgO BL/Ag (BL_s). Columns III to VIII refer, respectively, to cluster height with respect to the basal plane (h, Å), cluster diameter (d, Å), magnetization (μ, μ_B), Bader charge (Q, |e|), interfacial dipole moment (dip, |e|× Å), and adsorption energy (E_{ads}, eV).

I Support	II Ni_x	III h (Å)	IV d (Å)	V μ (μ_B)	VI Q (|e|)	VII dip (|e|× Å)	VIII E_{ads} (eV)
Gas-phase	13	-	4.67	8.00	-	-	-
	55	-	9.24	39.94	-	-	-
	147	-	13.93	99.19	-	-	-
ML_c	13	5.68	4.80	8.97	-0.11	-3.46	-5.39
	55	9.38	9.23	36.63	-0.89	-1.50	-8.46
	147	13.42	13.95	96.58	-1.47	+0.03	-12.12
ML_i	13	3.62	4.79	8.67	-0.02	-1.32	-5.10
	55	9.39	9.29	37.87	-0.67	+0.03	-7.25
	147	13.66	13.96	96.51	-1.07	+0.87	-9.65
BL_c	13	5.94	4.78	8.35	-0.27	-4.51	-5.14
	55	9.98	9.32	36.78	-1.63	-1.80	-7.78
	147	13.74	13.97	95.32	-2.55	+0.07	-11.37
BL_s	13	5.53	5.65	9.45	+0.10	-3.77	-8.22
	55	10.21	9.62	37.01	-1.30	-1.75	-9.71
	147	13.61	13.96	95.03	-2.22	-0.04	-15.39

Notably, a clear trend in the adsorption energy emerges for clusters of all sizes (Table 1, col. VIII): the strongest adhesion (corresponding to the most negative values of E_{ads}) is observed on the stepped BL, followed by the continuous ML, the continuous BL, and the stepped ML. This clearly shows the strong action as trapping sites exerted by the MgO steps. The stronger adhesion on continuous MLs compared to continuous BLs could be ascribed to two factors: i)

a stabilizing hybridization of the electron densities of the Ni atoms with the silver atoms, enabled by the extreme thinness of the MgO film, and ii) the larger work function of the continuous MgO ML/Ag compared to MgO BL/Ag, which could affect the charge injection to the Ni particle, strengthening the bond. The stronger binding of metal species on ML compared to BL has been previously observed for single atoms.[63] Finally, it is worth noting that the MgO ML/Ag interface is not an efficient trapping site. Indeed, all the clusters show the lowest E_{ads} on the ML_i substrate. Probably the stronger bonding between the truncated ML borders and the Ag substrate reduces site reactivity with respect to the stepped BL. We remark, however, that the BL_s model best reproduces our experimental conditions at step sites, where a monolayer MgO film covers both the top and the bottom terraces at the steps, with no Ag exposed.

Therefore, our calculations predict that the model of Fig. 2d is the most stable among the investigated ones, and Ni clusters are expected to decorate MgO steps. However, this result contrasts with the experimental data, showing a significant population of terraces at T≤250 K. The failure of the model in reproducing the experimental results indicates that an important parameter has been overlooked. Considering the role of interfacial oxygen in the growth of ordered MgO monolayers and in the spontaneous oxidation of ultrasmall Ni clusters, we focused our attention on the presence of O_{int}, and we included it in the calculations.[28-32]

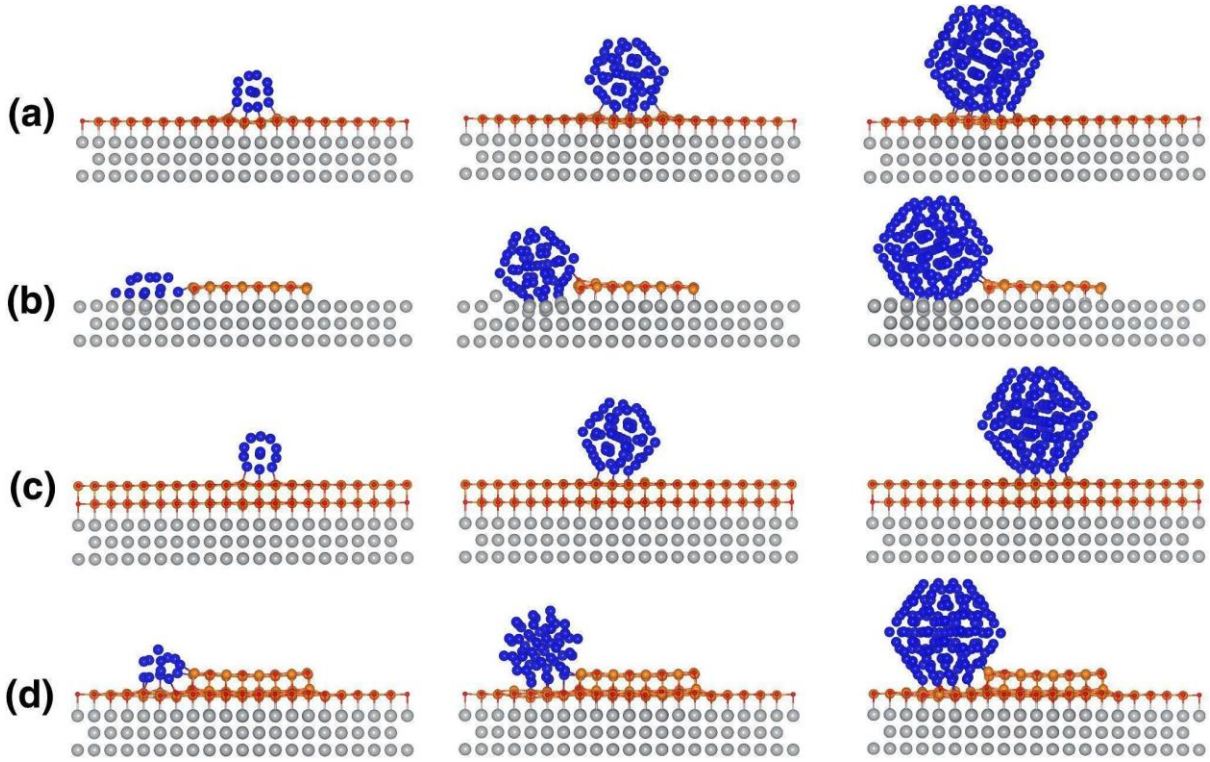


Figure 2. Side views of the calculated structures of Ni clusters on a) ML_c, b) ML_i, c) BL_c, d) BL_s.

4. Effect of the interfacial oxygen and clusters oxidation

The effect of adding oxygen at the interface in the computational models is shown in Fig.3 and Table 2 for the three most interesting cases previously described: continuous ML (ML_c_O), continuous BL (BL_c_O), and stepped BL (BL_s_O). In the models we assume 25% coverage of interfacial oxygen, corresponding to the optimal concentration reported in our previous work.[30] Partial oxidation of the Ni atoms in contact with the MgO film occurs, leading to global stabilization of the clusters, an effect that is more pronounced for the smallest nanoparticles. The observed clusters are indeed compatible with the presence of an oxide root as shown in the Supporting Material (Fig. S3).

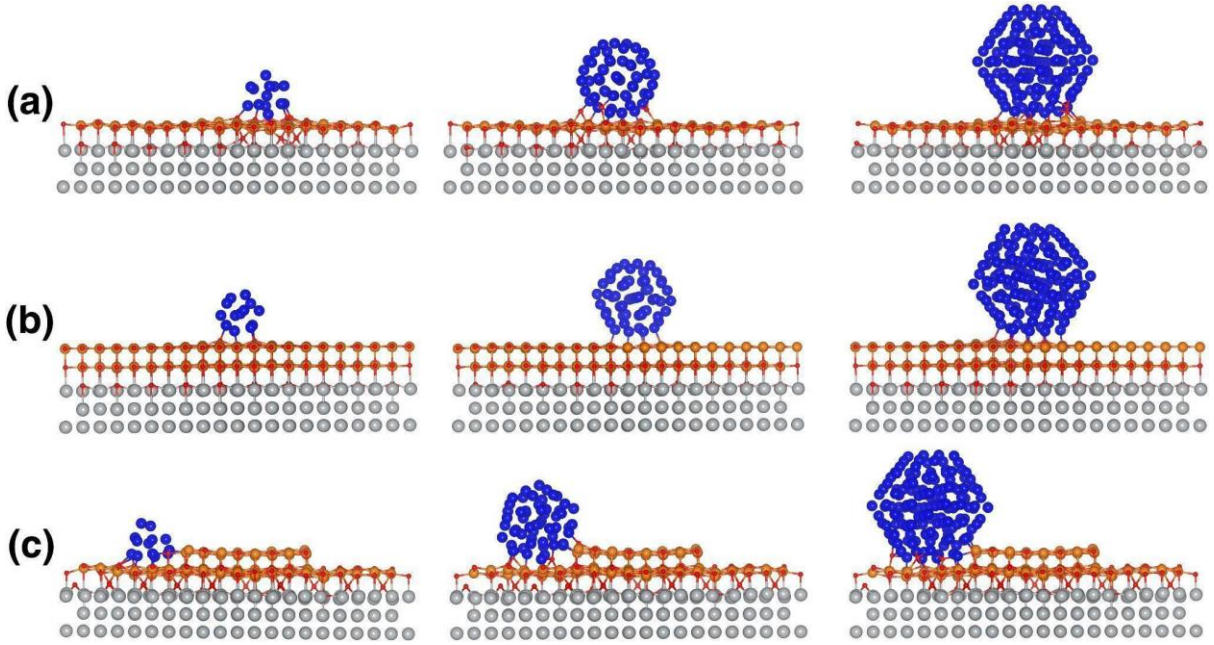


Figure 3. Side views of the calculated structures of Ni clusters on a) ML_c_O, b) BL_c_O, c) BL_s_O.

The data in Table 2 highlight the strong effect of O_{int} on the MgO surface physical and chemical properties and on the MgO interaction with Ni clusters. In particular, the main structural parameters of the adsorbed Ni_X are only marginally affected: comparing Table 1 and Table 2 one can notice only a negligible or small decrease in the physical height of the clusters (col. III). Vice versa, relevant changes are observed in the electronic and magnetic properties, as well as the adhesion strength and relative stability on the various supports. In general, the magnetization of Ni_X (col. V) is significantly larger on supports bearing 25% O_{int}, in particular on ML_c_O and BL_s_O. For the continuous MgO bilayer (BL_c_O), the effect is less pronounced. The change in the magnetization is related to an inversion of the charge state of the supported clusters that display negative charge on ML_c and BL_s (Table 1, col. VI) and positive (and generally larger) charge on ML_c_O and BL_s_O (Table 2, col. VI), in agreement with previous findings by some of us.[34] Interestingly, the effect is much smaller on BL_c_O, where the charge of the supported Ni clusters is negative (though less negative than in the

absence of O_{int}, Table 1) or almost neutral. Steps, thus, represent an intermediate case between ML terraces, where the stabilization exerted by O_{int} on metal clusters is very strong, and BL terraces, where the effect is very weak.

In general, in the presence of interfacial oxygen, the adsorption energy is remarkably larger on all types of MgO supports (Table 2, col. VIII). However, this enhancement in stability is much stronger in ML_c_O than in MgO bilayers and it affects the overall stability trend. Indeed, in the presence of interfacial oxygen, the clusters are bound more strongly on continuous ML terraces (ML_c_O) than at bilayer steps (BL_s_O) and this behaviour is opposite to the one predicted in the absence of Oint (compare ML_c and BL_s in Table 1, col. VIII).

The different effect of an analogous concentration of interfacial oxygen on MgO MLs and BLs can be attributed to the different thickness of the insulating MgO layers. As expected, the effect of O_{int} is smaller on thicker BLs compared to MLs.

Table 2. Ni_X (X=13, 55, 147) adsorbed on MgO/O/Ag (bearing 25% O_{int} at the MgO/Ag interface). Calculated values for the continuous MgO ML/O/Ag (ML_c_O), continuous MgO BL/O/Ag (BL_c_O), and stepped BL/O/Ag (BL_s_O) supports are reported. Columns III to VIII refer, respectively, to cluster height with respect to the basal plane (h, Å), cluster diameter (d, Å), cluster magnetization (μ, μ_B), Bader charge (Q, |e|), interfacial dipole moment (dip, |e|× Å), and adsorption energy (E_{ads}, eV).

I	II	III	IV	V	VI	VII	VIII
Support	**Ni_x**	**h (Å)**	**d (Å)**	**μ (μ_B)**	**Q (|e|)**	**dip (|e|× Å)**	**E_{ads} (eV)**
ML_c_O	13	5.47	4.77	10.69	+0.91	-1.42	-23.36
	55	9.12	9.27	40.14	+1.78	-0.57	-28.77
	147	13.20	13.96	100.14	+1.92	+0.55	-32.65
BL_c_O	13	6.02	4.86	9.58	+0.48	-2.08	-8.22
	55	9.79	9.31	37.96	-0.08	-0.62	-7.95
	147	13.66	14.02	97.86	-0.02	+0.32	-11.91
BL_s_O	13	5.63	6.15	11.79	+1.41	-0.52	-15.53
	55	10.17	9.67	38.93	+1.33	+0.19	-17.28
	147	11.52	14.42	97.29	+1.91	+0.87	-23.12

We can now explain the effect of deposition temperature on the cluster distribution observed in the STM experiments using these DFT results. Firstly, we recall that Ni clusters on monolayer MgO terraces are best modelled by Ni_X adsorption at the ML_c or ML_c_O

supports, whereas BL_s or BL_s_O are more suitable for representing cluster adsorption at the MgO steps. DFT clearly indicates the essential role of interface oxygen concentration and of its temperature dependence. Indeed, the presence of aggregations larger than few-atoms at 100 K already, in agreement with previous reports [33], is a key-point in indicating the presence of a mechanism acting beyond bare thermally enhanced diffusion. On the other hand, theory predicts that, in the absence of interfacial oxygen, the Ni clusters are most stably adsorbed at MgO steps of the BL_s supports. In contrast, in the presence of O_{int}, partial oxidation and adsorption on ML terraces (ML_c_O) is favoured.

Therefore, we can rationalize the different spatial distribution of Ni clusters vs growth temperature considering that for T≤250 K there is enough interfacial oxygen for the clusters to get partially oxidized and anchor at terraces; vice versa, at T=300 K the O_{int} concentration is depleted and MgO steps become the most favourable adsorption site.

This picture is supported by the calculation of the O_{int} free energy at $P=1 \times 10^{-9}$ mbar and T=100-400 K (see Table S2 in the Supporting Material), i.e. in conditions close to the experimental ones for Ni clusters growth. At 25% O_{int} coverage, Ni NCs are stable on all supports, with a trend in binding energy that is ML_c ≈ BL_c > BL_s. However, the adsorption energy values decrease with increasing temperature, becoming almost negligible at 400 K. Experimentally, an estimate of O_{int} is available only at 200 K but, considering that comparison with DFT calculations are only qualitative, it is reasonable to suppose that the stability of O_{int} is negligible already at RT.[28] It is also interesting, in this respect, to mention that the different O_{int} stability in ML_c and BL_c (i.e. in the central region of MgO islands) compared to steps could induce oxygen diffusion within the MgO/Ag interface. Overall, the O_{int} concentration can vary due to various factors; direct evaporation of oxygen is unlikely under the observed experimental conditions but reverse oxygen spillover or diffusion into the subsurface Ag(100) region must be considered. Reverse oxygen spillover from the MgO/Ag interface to the external surfaces of the adsorbed Ni clusters was recently proved to be strongly thermodynamically favoured for Ni_{55} clusters by DFT calculations. It implies a concerted mechanism in which O atoms from the MgO lattice move to the Ni cluster borders and the oxygen vacancies are refilled by interfacial oxygen species.[34] It was not possible, though, to evaluate the actual diffusion barrier for this process. From the experimental point of view, the deposition of Ni adatoms takes place in ultrahigh vacuum so that O_{int} is the only oxygen reservoir available for the observed formation of NiO_x clusters.[32] It is thus possible that, in the initial stage of nucleation and growth of the clusters, concomitant partial oxidation takes place, as also supported by the analysis of the shapes and height profiles in the STM images reported in the Supporting Material, and the occasional identification of the previously described Ni_xO_y oligomers.[32] At higher temperatures, the kinetic barriers hindering this mechanism will be more easily overcome. This effect, combined with the higher mobility of deposited Ni atoms, contributes to explaining the change in the clusters' size and spatial distribution observed at room temperature. The diffusion of partially oxidized Ni_xO_y entities could, in principle, also contribute to further non-trivial growth mechanisms.

The diffusion of the interfacial oxygen back into the Ag subsurface is difficult to monitor experimentally. Some of us demonstrated, using photoelectron spectroscopy, that a subsurface

oxygen species migrates into the bulk at T > 280 K on O/Ag(210).[64] However, the situation is different if oxygen is trapped at the MgO/Ag interface, so that we must rely on DFT calculations showing that diffusion into the Ag bulk is thermodynamically unfavourable (see Supporting Maerial, Fig. S4). The most probable fate of the subsurface oxygen is therefore its migration into the larger Ni clusters forming at RT.

Finally, we remark that the diffusion barrier for such clusters is expected to be around 1/3 of their adsorption energy, which implies that they should not sinter at temperatures lower than 600 K. This agrees well with the size distribution of the grown nanoparticles, having a diameter between 1.0 and 1.5 nm, i.e. compatible with the size of Ni_{55} and Ni_{147}, and demonstrates the active role of a suitable substrate in the optimization of catalytic materials.[33] This result is potentially quite appealing to obtain nanoparticles of kinetically limited shape under temperature conditions which are considered the optimal ones for CO_2 methanation on non-reducible oxide supports (640 K according to ref. [10]). It must be stated, though, that the catalytic operating conditions do not envisage only high temperature, but also exposure to high pressure of reactive gases such as oxygen, hydrogen, CO_2 and others. Our previous computational work [34] assesses the stability of supported Ni clusters in an oxidizing environment, but their behaviour under reducing conditions and exposure to reactive gases remains to be investigated.

5. Conclusions

In this study we show that the nucleation, spatial distribution and thermal stability of Ni nanoclusters on MgO/Ag(100) surfaces are strongly influenced by the morphology of the substrate by using STM analysis and DFT calculations.

The MgO/Ag interface acts as a reservoir releasing O in oxygen poor conditions or segregating it under oxygen rich conditions. The observed nucleation pattern highlights the combined role of interfacial oxygen and diffusion kinetics in directing cluster growth. Furthermore, stability analysis reveals that Ni clusters retain their structural integrity within a definite size regime, while the migration to steps observed at 300 K could further lead to agglomeration. These results provide fundamental insights into metal oxide/interface behaviour and open pathways for tailoring Ni NCs for catalysis and nanoscale devices.

Acknowledgements

We thank Jagriti Pal for participating in the initial stages of STM experiments.

We acknowledge funding from the European Union – NextGenerationEU, Mission 4, Component 1, through the Italian Ministry of University and Research under projects PRIN-PNRR P20227XSAH, CUP B53D23028390001 and project PRIN 2022 2022LS74H2, CUP B53D23013810006.

Computational support from CINECA supercomputing centre is kindly acknowledged.

Author Contributions. Conceptualization: S.T., M.R. L.S.; methodology and formal analysis: A.S. L.S., M.J.V., S.T.; investigation: all authors; Funding acquisition: S.T., L.S., M.R.; data curation: A.S. L.S., M.J.V., S.T.; writing—original draft preparation: A.S. L.S., M.J.V., S.T, M.R., writing—review and editing: all authors. All authors have read and agreed to the published version of the manuscript.

Conflicts of Interest: The authors declare no conflicts of interest.

References

[1] M. Monai, M. Gambino, S. Wannakao, B.M. Weckhuysen, Propane to olefins tandem catalysis: a selective route towards light olefins production, Chemical Society Reviews 50(20) (2021) 11503-11529.

[2] J. Gong, R. Luque, Catalysis for production of renewable energy, Chemical Society Reviews 43(22) (2014) 7466-7468.

[3] J.R. Lockemeyer, T.L. Lohr, M.A. Reynolds, A. van der Made, Catalysis for the Energy Transition, ChemCatChem (2025) e00588.

[4] G. Centi, J. Čejka, Needs and gaps for catalysis in addressing transitions in chemistry and energy from a sustainability perspective, ChemSusChem 12(3) (2019) 621-632.

[5] I. Chorkendorff, J.W. Niemantsverdriet, Concepts of modern catalysis and kinetics, John Wiley & Sons, 2017.

[6] Y. Xia, H. Yang, C.T. Campbell, Nanoparticles for catalysis, ACS Publications, (2013), pp. 1671-1672.

[7] D. Astruc, Introduction: nanoparticles in catalysis, ACS Publications, 2020, pp. 461-463.

[8] U. Heiz, E.L. Bullock, Fundamental aspects of catalysis on supported metal clusters, Journal of Materials Chemistry 14(4) (2004) 564-577.

[9] E. Bus, R. Prins, J.A. van Bokhoven, Origin of the cluster-size effect in the hydrogenation of cinnamaldehyde over supported Au catalysts, Catalysis Communications 8(9) (2007) 1397-1402.

[10] E.B. Sterk, A.-E. Nieuwelink, M. Monai, J.N. Louwen, E.T. Vogt, I.A. Filot, B.M. Weckhuysen, Structure sensitivity of CO2 conversion over nickel metal nanoparticles explained by micro-kinetics simulations, JACS Au 2(12) (2022) 2714-2730.

[11] O. Dulub, W. Hebenstreit, U. Diebold, Imaging cluster surfaces with atomic resolution: the strong metal-support interaction state of Pt supported on TiO_2(110), Physical Review Letters 84(16) (2000) 3646.

[12] S. Tauster, Strong metal-support interactions, Accounts of Chemical Research 20(11) (1987) 389-394.

[13] Z.-H. Qin, M. Lewandowski, Y.-N. Sun, S. Shaikhutdinov, H.-J. Freund, Morphology and CO adsorption on platinum supported on thin Fe3O4(111) films, Journal of Physics: Condensed Matter 21(13) (2009) 134019.

[14] M. Lewandowski, Y.-N. Sun, Z.-H. Qin, S. Shaikhutdinov, H.-J. Freund, Promotional effect of metal encapsulation on reactivity of iron oxide supported Pt catalysts, Applied Catalysis A: General 391(1-2) (2011) 407-410.

[15] J.Y. Park, L.R. Baker, G.A. Somorjai, Role of hot electrons and metal–oxide interfaces in surface chemistry and catalytic reactions, Chemical Reviews 115(8) (2015) 2781-2817.

[16] T. Lunkenbein, J. Schumann, M. Behrens, R. Schlögl, M.G. Willinger, Formation of a ZnO overlayer in industrial Cu/ZnO/Al2O3 catalysts induced by strong metal–support interactions, Angewandte Chemie 127(15) (2015) 4627-4631.

[17] F. Polo-Garzon, T.F. Blum, Z. Bao, K. Wang, V. Fung, Z. Huang, E.E. Bickel, D.-e. Jiang, M. Chi, Z. Wu, In situ strong metal–support interaction (SMSI) affects catalytic alcohol conversion, ACS Catalysis 11(4) (2021) 1938-1945.

[18] J.A. Farmer, C.T. Campbell, Ceria maintains smaller metal catalyst particles by strong metal-support bonding, Science 329(5994) (2010) 933-936.

[19] T. Zambelli, J. Wintterlin, J. Trost, G. Ertl, Identification of the" active sites" of a surface-catalyzed reaction, Science 273(5282) (1996) 1688-1690.

[20] N. Nilius, Properties of oxide thin films and their adsorption behavior studied by scanning tunneling microscopy and conductance spectroscopy, Surface Science Reports 64(12) (2009) 595-659.

[21] S. Street, C. Xu, D. Goodman, The physical and chemical properties of ultrathin oxide films, Annual Review of Physical Chemistry 48(1) (1997) 43-68.

[22] J.M. Rondinelli, N.A. Spaldin, Structure and properties of functional oxide thin films: insights from electronic-structure calculations, Advanced Materials 23(30) (2011) 3363-3381.

[23] L. Giordano, G. Pacchioni, Oxide films at the nanoscale: new structures, new functions, and new materials, Accounts of Chemical Research 44(11) (2011) 1244-1252.

[24] G. Pacchioni, H. Freund, Electron transfer at oxide surfaces. The MgO paradigm: from defects to ultrathin films, Chemical Reviews 113(6) (2013) 4035-4072.

[25] D. Ricci, A. Bongiorno, G. Pacchioni, U. Landman, Bonding Trends and Dimensionality Crossover of Gold Nanoclusters on Metal-Supported MgO Thin Films, Physical Review Letters 97(3) (2006) 036106.

[26] F. Calaza, C. Stiehler, Y. Fujimori, M. Sterrer, S. Beeg, M. Ruiz-Oses, N. Nilius, M. Heyde, T. Parviainen, K. Honkala, Carbon dioxide activation and reaction induced by electron transfer at an oxide–metal interface, Angewandte Chemie International Edition 54(42) (2015) 12484-12487.

[27] E. Carrasco, M.A. Brown, M. Sterrer, H.-J. Freund, K. Kwapien, M. Sierka, J. Sauer, Thickness-dependent hydroxylation of MgO(001) thin films, The Journal of Physical Chemistry C 114(42) (2010) 18207-18214.

[28] J. Pal, M. Smerieri, E. Celasco, L. Savio, L. Vattuone, M. Rocca, Morphology of monolayer MgO films on Ag (100): switching from corrugated islands to extended flat terraces, Physical Review Letters 112(12) (2014) 126102.

[29] N. Janulaitis, C.T. Campbell, Predicting Adhesion Energies of Late Transition Metal Nanoparticles to Oxide Support Surfaces Using Oxide Reducibility and Metal Oxophilicity: Toward Predicting Catalyst Performance, ACS Catalysis 15(9) (2025) 6874-6880.

[30] J. Pal, M. Smerieri, E. Celasco, L. Savio, L. Vattuone, R. Ferrando, S. Tosoni, L. Giordano, G. Pacchioni, M. Rocca, How growing conditions and interfacial oxygen affect the final morphology of MgO/Ag(100) films, The Journal of Physical Chemistry C 118(45) (2014) 26091-26102.

[31] L. Savio, M. Smerieri, L. Vattuone, S. Tosoni, G. Pacchioni, M. Rocca, Interface Oxygen Induced Internal Structures of Ultrathin MgO Islands Grown on Ag(100), The Journal of Physical Chemistry C 124(16) (2020) 8834-8842.

[32] M. Smerieri, J. Pal, L. Savio, L. Vattuone, R. Ferrando, S. Tosoni, L. Giordano, G. Pacchioni, M. Rocca, Spontaneous oxidation of Ni nanoclusters on MgO monolayers induced by segregation of interfacial oxygen, The Journal of Physical Chemistry Letters 6(15) (2015) 3104-3109.

[33] L. Savio, M. Smerieri, J. Pal, E. Celasco, M. Rocca, L. Vattuone, 2D Ni Nanoclusters on Ultrathin MgO/Ag(100), The Journal of Physical Chemistry C 124(1) (2019) 482-488.

[34] M. Jahangirzadeh Varjovi, S. Tosoni, DFT Investigation of X55 (X= Ni, Pd, and Pt) Clusters on Ultrathin Supported MgO Films: Evidence of Oxygen Spillover and Relevance for Catalytic Model Studies, The Journal of Physical Chemistry C 128(50) (2024) 21331-21342.

[35] W. Gac, T. Borowiecki, P. Kowalik, Nickel Nanocatalysts for Methane Steam Reforming, Nanotechnology in Catalysis: Applications in the Chemical Industry, Energy Development, and Environment Protection (2017) 401-420.

[36] A. Parmaliana, F. Arena, F. Frusteri, S. Coluccia, L. Marchese, G. Martra, A. Chuvilin, Magnesia-supported nickel catalysts: II. Surface properties and reactivity in methane steam reforming, Journal of Catalysis 141(1) (1993) 34-47.

[37] S. Schauermann, N. Nilius, S. Shaikhutdinov, H.-J. Freund, Nanoparticles for heterogeneous catalysis: new mechanistic insights, Accounts of Chemical Research 46(8) (2013) 1673-1681.

[38] A. Cadi-Essadek, A. Roldan, X. Aparicio-Anglès, N.H. De Leeuw, CO_2 and H_2 adsorption and reaction at Nin/YSZ(111) interfaces: a density functional theory study, The Journal of Physical Chemistry C 122(34) (2018) 19463-19472.

[39] G.I. Siakavelas, N.D. Charisiou, S. AlKhoori, A.A. AlKhoori, V. Sebastian, S.J. Hinder, M.A. Baker, I. Yentekakis, K. Polychronopoulou, M.A. Goula, Highly selective and stable nickel catalysts supported on ceria promoted with Sm_2O_3, Pr_2O_3 and MgO for the CO_2 methanation reaction, Applied Catalysis B: Environmental 282 (2021) 119562.

[40] C.R. Rêgo, P. Tereshchuk, L.N. Oliveira, J.L. Da Silva, Graphene-supported small transition-metal clusters: A density functional theory investigation within van der Waals corrections, Physical Review B 95(23) (2017) 235422.

[41] W.-S. Dong, K.-W. Jun, H.-S. Roh, Z.-W. Liu, S.-E. Park, Comparative study on partial oxidation of methane over Ni/ZrO_2, Ni/CeO_2 and $Ni/Ce–ZrO_2$ catalysts, Catalysis Letters 78(1) (2002) 215-222.

[42] A. Caballero, J.P. Holgado, V.M. Gonzalez-delaCruz, S.E. Habas, T. Herranz, M. Salmeron, In situ spectroscopic detection of SMSI effect in a Ni/CeO_2 system: hydrogen-induced burial and dig out of metallic nickel, Chemical Communications 46(7) (2010) 1097-1099.

[43] G.G. Asara, L.O. Paz-Borbón, F. Baletto, "Get in Touch and Keep in Contact": Interface effect on the oxygen reduction reaction (ORR) activity for supported PtNi nanoparticles, ACS Catalysis 6(7) (2016) 4388-4393.

[44] C.T. Campbell, The energetics of supported metal nanoparticles: relationships to sintering rates and catalytic activity, Accounts of Chemical Research 46(8) (2013) 1712-1719.

[45] F.C. Henn, M.E. Bussell, C.T. Campbell, A simple means for reproducibly dosing low vapor pressure and/or reactive gases to surfaces in ultrahigh vacuum, Journal of Vacuum Science & Technology A: Vacuum, Surfaces, and Films 9(1) (1991) 10-13.

[46] I. Horcas, R. Fernández, J. Gomez-Rodriguez, J. Colchero, J. Gómez-Herrero, A.M. Baro, WSXM: A software for scanning probe microscopy and a tool for nanotechnology, Review of Scientific Instruments 78(1) (2007).

[47] W. Kohn, L.J. Sham, Self-consistent equations including exchange and correlation effects, Physical Review 140(4A) (1965) A1133.

[48] P. Hohenberg, W. Kohn, Density functional theory (DFT), Phys. Rev 136(1964) (1964) B864.

[49] S. Schintke, S. Messerli, M. Pivetta, F. Patthey, L. Libioulle, M. Stengel, A. De Vita, W.-D. Schneider, Insulator at the ultrathin limit: MgO on Ag (001), Physical Review Letters 87(27) (2001) 276801.

[50] G. Kresse, J. Hafner, Ab initio molecular dynamics for liquid metals, Physical Review B 47(1) (1993) 558.

[51] G. Kresse, J. Hafner, Ab initio molecular-dynamics simulation of the liquid-metal–amorphous-semiconductor transition in germanium, Physical Review B 49(20) (1994) 14251.

[52] G. Kresse, J. Furthmüller, Efficiency of ab-initio total energy calculations for metals and semiconductors using a plane-wave basis set, Computational Materials Science 6(1) (1996) 15-50.

[53] G. Kresse, J. Furthmüller, Efficient iterative schemes for ab initio total-energy calculations using a plane-wave basis set, Physical Review B 54(16) (1996) 11169.

[54] J.P. Perdew, K. Burke, M. Ernzerhof, Generalized gradient approximation made simple, Physical Review Letters 77(18) (1996) 3865.

[55] P.E. Blöchl, Projector augmented-wave method, Physical review B 50(24) (1994) 17953.

[56] H.J. Monkhorst, J.D. Pack, Special points for Brillouin-zone integrations, Physical Review B 13(12) (1976) 5188.

[57] G. Henkelman, A. Arnaldsson, H. Jónsson, A fast and robust algorithm for Bader decomposition of charge density, Computational Materials Science 36(3) (2006) 354-360.

[58] S. Grimme, S. Ehrlich, L. Goerigk, Effect of the damping function in dispersion corrected density functional theory, Journal of Computational Chemistry 32(7) (2011) 1456-1465.

[59] S. Grimme, J. Antony, S. Ehrlich, H. Krieg, A consistent and accurate ab initio parametrization of density functional dispersion correction (DFT-D) for the 94 elements H-Pu, The Journal of Chemical Physics 132(15) (2010).

[60] T.E. James, S.L. Hemmingson, C.T. Campbell, Energy of supported metal catalysts: from single atoms to large metal nanoparticles, ACS Catalysis 5(10) (2015) 5673-5678.

[61] T. Hynninen, G. Cabailh, A.S. Foster, C. Barth, Defect mediated manipulation of nanoclusters on an insulator, Scientific Reports 3(1) (2013) 1270.

[62] T. Rapps, R. Ahlrichs, E. Waldt, M.M. Kappes, D. Schooss, On the structures of 55-atom transition-metal clusters and their relationship to the crystalline bulk, Angewandte Chemie International Edition 52(23) (2013).

[63] S. Tosoni, G. Pacchioni, Bonding Properties of Isolated Metal Atoms on Two-Dimensional Oxides, The Journal of Physical Chemistry C 124(38) (2020) 20960-20973.

[64] L. Savio, A. Gerbi, L. Vattuone, A. Baraldi, G. Comelli, M. Rocca, Monitoring super-and subsurface oxygen on Ag (210) by high energy resolution X-ray photoelectron spectroscopy: Subsurface diffusion and segregation, The Journal of Physical Chemistry B 110(2) (2006) 942-947.

Supporting Information

The role of interfacial oxygen in the nucleation and stability of Ni Nanoclusters at MgO ultrathin films: insights from STM and first-principles DFT calculations

Mirali Jahangirzadeh Varjovi[1*], Anshika Singh[2*], Elina Mkrtchian[3,4], Mario Rocca[2,3], Luca Vattuone[2,3], Letizia Savio[3#], Sergio Tosoni[1#]

[1]*Department of Materials Science, University of Milano-Bicocca, 20125 Milano, Italy*

[2]*Department of Physics, University of Genova, via Dodecaneso 33, 16146 Genova, Italy*

[3]*IMEM-CNR, UOS Genova, via Dodecaneso 33, 16146 Genova, Italy*

[4]*Department of Mathematical, Physical and Computer Sciences, University of Parma, 43124 Parma, Italy*

* *These authors contributed equally*

\# *Corresponding authors: sergio.tosoni@unimib.it, letizia.savio@cnr.it*

Table S1: Distribution of Ni nanoclusters at MgO step or terrace sites. From left to right, the columns refer to the deposition temperature of Ni atoms, to the number of STM overviews (typically 26 nm x 26 nm in size) used for the analysis and to the percentage of Ni NCs found at steps and at terrace sites.

T (K)	Number of images	Average population at steps (%)	Average population at terraces (%)
100	10	32±3	68±3
200	13	24±2	76±2
250	5	20±5	80±5
300	11	89±3	11±3

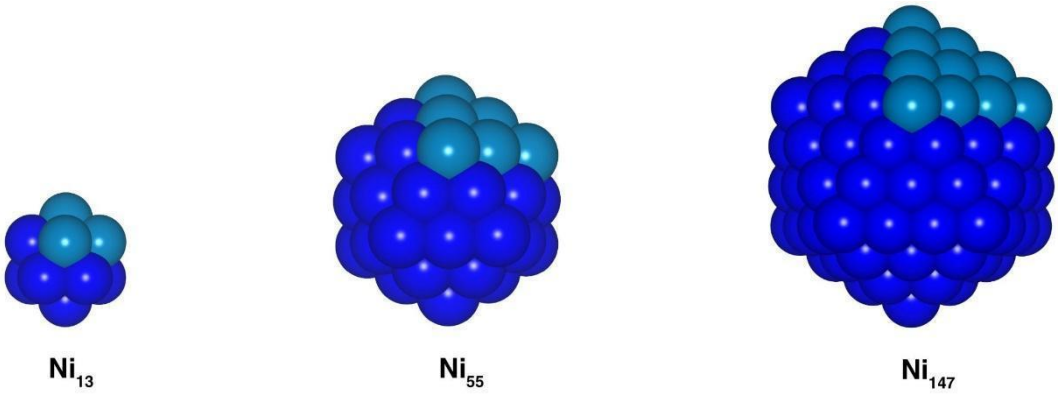


Fig. S1. Free standing Ni nanoclusters

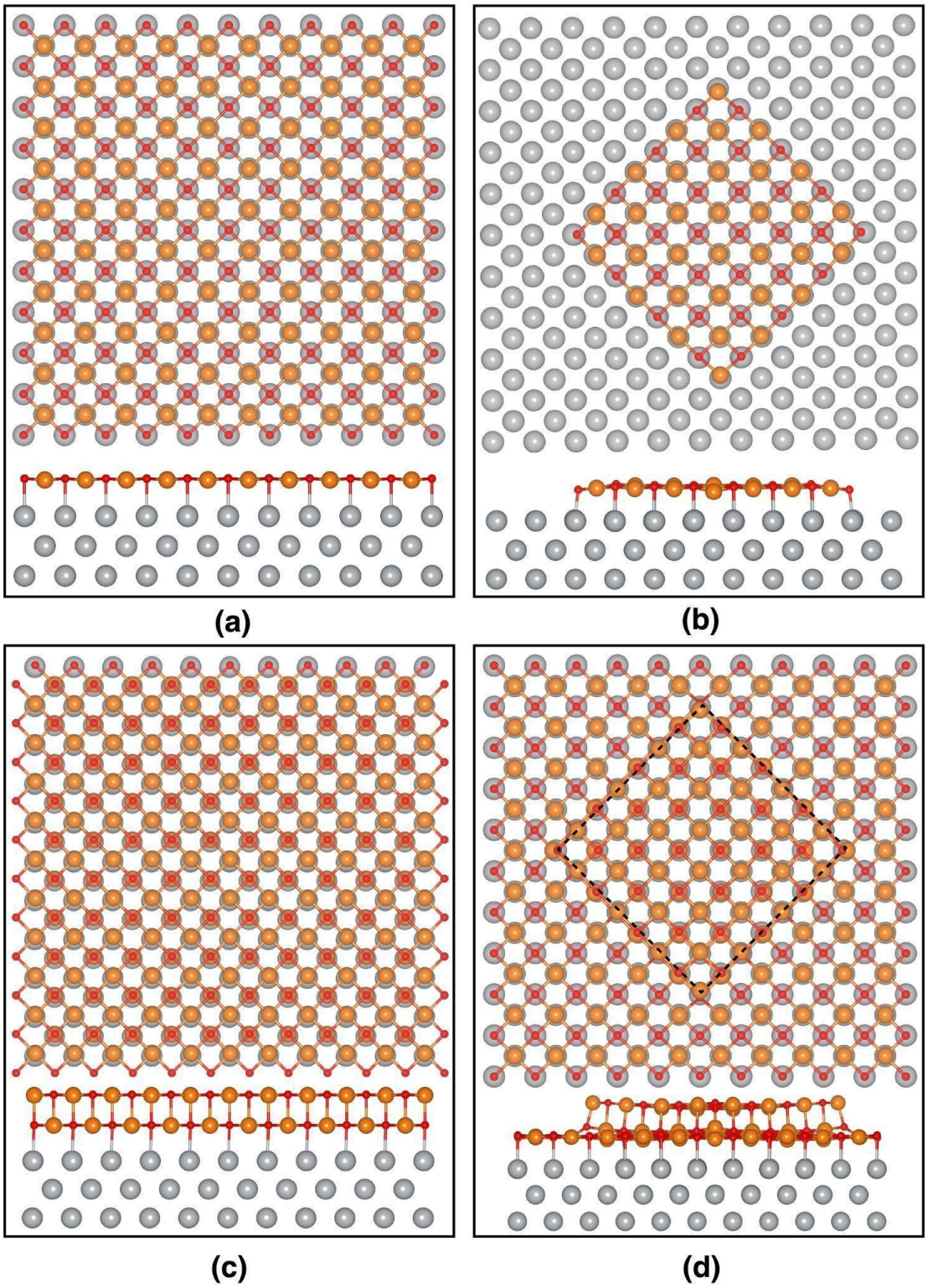


Fig. S2. Various types of MgO supports considered in this work: a) continuous ML (ML_c) b) finite ML island (ML_i) c) continuous BL (BL_c) d) stepped BL (BL_s).

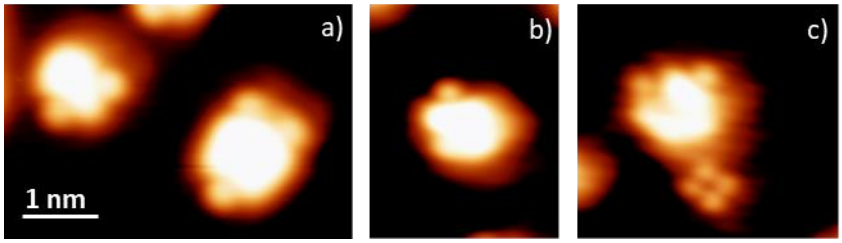


Fig. S3. Examples of "exotic" Ni nanoclusters observed after deposition on 1 ML MgO/Ag(100) at 200 K. The separate lobes present at the periphery of each nanoparticle are compatible with the partial oxidation of a few Ni atoms of the cluster, reasonably at the Ni/MgO interface. The cluster in panel c) also shows a fully oxidized Ni tetramer as those already discussed in ref. [1]

Table S2. O_{int} binding free energy (eV per O atom) at $P=1\times10^{-9}$ mbar and T=100-400 K (mimicking the experimental growth conditions). The O_{int} loading is 25%.

Support	T= 100 K	T= 200 K	T= 300 K	T= 350 K	T= 400 K
ML_c	-0.70	-0.49	-0.28	-0.17	-0.05
BL_c	-0.68	-0.47	-0.25	-0.14	-0.02
BL_s	-0.56	-0.35	-0.13	-0.02	+0.09

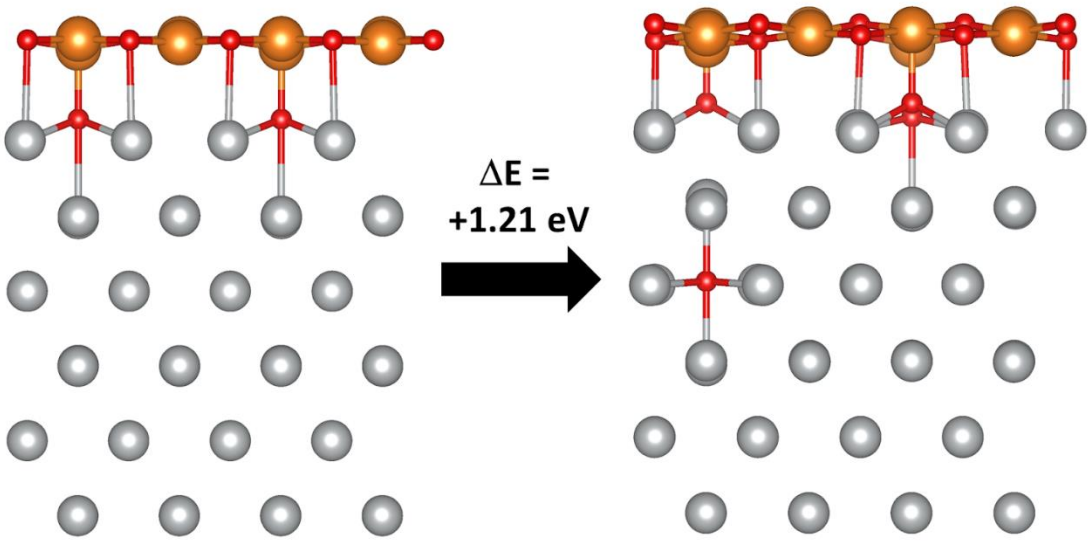
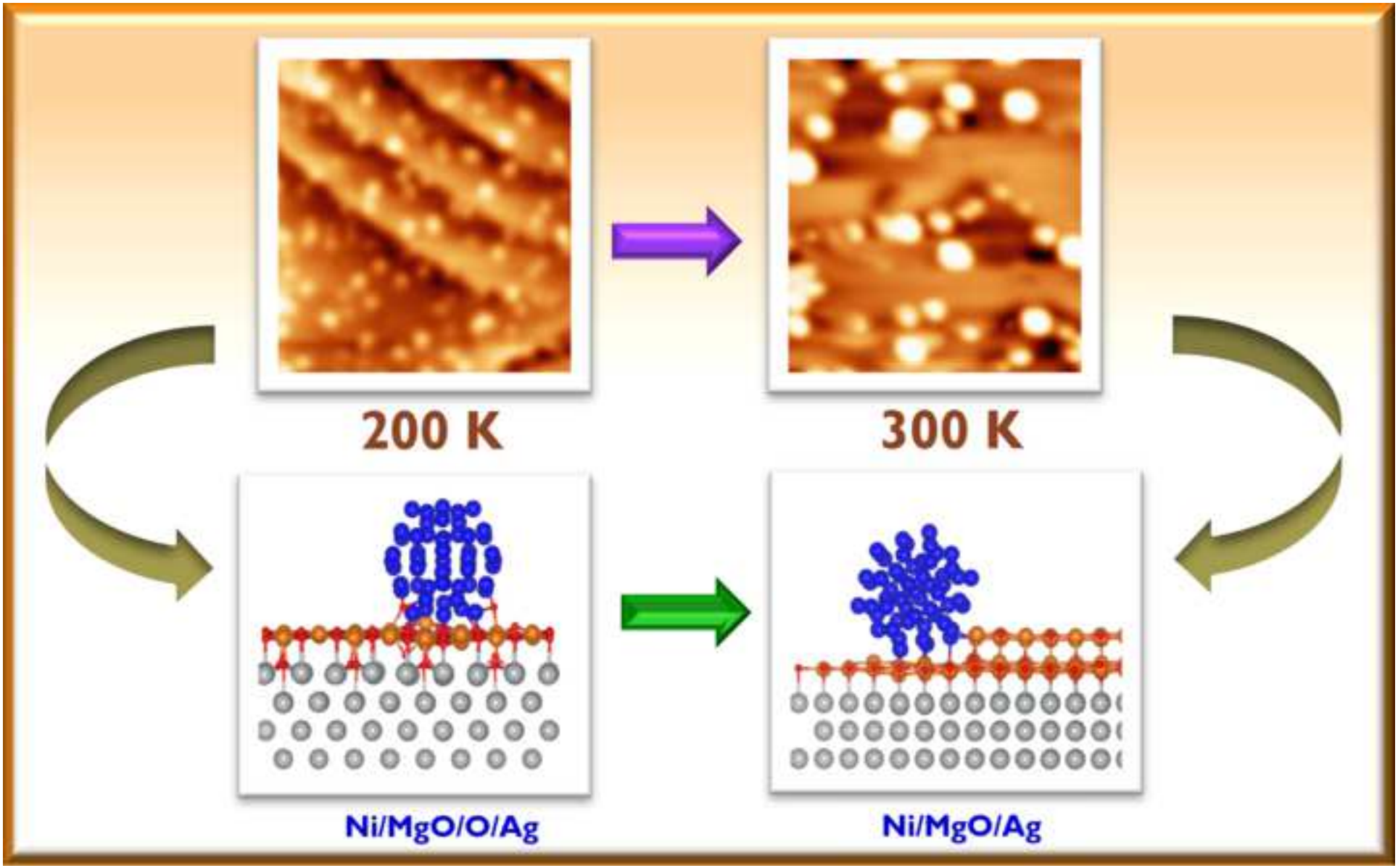


Fig. S4. Simulation of the diffusion of an oxygen atom from the MgO/Ag interface to the Ag bulk. To this aim, the thickness of the Ag slab was increased to 6 layers (only the bottom layer is fixed at the bulk position during the structure relaxations) and a 4x4 supercell was adopted. The O_{int} loading in the starting structure (left panel) is 25%.

References

[1] M. Smerieri, J. Pal, L. Savio, L. Vattuone, R. Ferrando, S. Tosoni, L. Giordano, G. Pacchioni, M. Rocca, Spontaneous Oxidation of Ni Nanoclusters on Mgo Monolayers Induced by Segregation of Interfacial Oxygen. *The Journal of Physical Chemistry Letters* **6**, 3104-3109 (2015).

Click here to access/download;Graphical Abstract (for review);TOC.tif



The corresponding author hereby gives credit to all co-authors for their contributions to the manuscript entitled “The role of interfacial oxygen in the nucleation and stability of Ni nanoclusters at MgO ultrathin films: Insights from STM and first-principles DFT calculations”.

All authors agreed to submission of the manuscript, in its present form, to the journal “Surfaces and Interfaces”.

Mirali Jahangirzadeh Varjovi: methodology and formal analysis, investigation, data curation, writing—original draft preparation, writing—review and editing.

Anshika Singh: methodology and formal analysis, investigation, data curation, writing—original draft preparation, writing—review and editing.

Elina Mkrtchian: investigation, writing—review and editing.

Mario Rocca: conceptualization, investigation, funding acquisition, writing—original draft preparation, writing—review and editing.

Luca Vattuone: investigation, writing—review and editing.

Letizia Savio: conceptualization, methodology and formal analysis, investigation, funding acquisition, data curation, writing—original draft preparation, writing—review and editing.

Sergio Tosoni: conceptualization, methodology and formal analysis, investigation, funding acquisition, data curation, writing—original draft preparation, writing—review and editing.

Revised Manuscript Marked

The role of interfacial oxygen in the nucleation and stability of Ni nanoclusters at MgO ultrathin films: Insights from STM and first-principles DFT calculations

Mirali Jahangirzadeh Varjovi[1*], Anshika Singh[2*], Elina Mkrtchian[3,4], Mario Rocca[2,3], Luca Vattuone[2,3], Letizia Savio[3#], Sergio Tosoni[1#]

[1]*Department of Materials Science, University of Milano-Bicocca, 20125 Milano, Italy*

[2]*Department of Physics, University of Genova, via Dodecaneso 33, 16146 Genova, Italy*

[3]*IMEM-CNR, UOS Genova, via Dodecaneso 33, 16146 Genova, Italy*

[4]*Department of Mathematical, Physical and Computer Sciences, University of Parma, 43124 Parma, Italy*

* *These authors contributed equally*

\# *Corresponding authors: sergio.tosoni@unimib.it, letizia.savio@cnr.it*

Abstract

The interaction between metal nanoclusters and oxide surfaces plays a crucial role in determining the properties of materials for catalytic and electronic applications. Here we present a combined experimental scanning tunnelling microscopy and first-principles calculations study of the nucleation and spatial distribution of Ni nanoclusters grown by deposition of Ni atoms on MgO monolayer films supported on Ag(100) at temperature between 100 K and 300 K. Clusters compatible in size with the magic number 13, 55 and 147 compact icosahedral structures are metallic, but partially oxidized in the contact area with the MgO film. They also show a markedly different spatial distribution with deposition temperature: up to 250 K they sit mainly on flat MgO terraces, while at 300 K they accumulate almost exclusively at the steps. Both effects are caused by the unavoidable presence of oxygen atoms at the MgO/Ag interface, whose concentration decreases dramatically just below room temperature.

1. Introduction

Catalysis plays a fundamental role in the production of goods and energy in contemporary society.[1] Its relevance is steadily increasing as the paradigm shifts toward circular pathways and the exploitation of renewable energy sources.[2-4] In particular, most employed catalytic systems fall under the definition of heterogeneous catalysts, in which the active species is a (more or less) small metal particle anchored on a solid support.[5-7] Reducing the size of a supported metal catalyst to the nanoscale is beneficial for saving precious raw materials, maximizing the mass/activity ratio, and increasing the catalyst activity.[8-9] E.g., a recent Density Functional Theory (DFT) and microkinetic study demonstrated that nickel nanoparticles with 1.7 nm size are expected to have the highest catalytic performance for CO_2 methanation.[10]

Catalytic reactions often occur at relatively high temperatures, where sintering may take place. The ability to control the size and the properties of supported nanoparticles is thus essential for further optimization of the heterogeneous catalyst. In this respect, the interaction with the

support plays a significant role. On the one hand, it ultimately controls the stability of the active particles and their tendency to undergo sintering and thermal deactivation.[11-17] Indeed, it was shown that Ag clusters stop sintering at a diameter of 6 nm on MgO but only of ~3 nm on Ceria.[18] On the other hand, chemical and structural changes induced by the support on the metal particles can deeply affect their chemical properties and reactivity.

It is thus interesting to complement applied studies in catalysis, where the activity and turnover frequency of a given system are the main figures of merit, with more basic works, aimed at the thorough characterization of the structural properties of supported metal nanoparticles and their interaction with the support. This eventually justified the effort to grow insulating oxides as ultrathin films on metal surfaces: such systems allow the study of wide-gap oxides (often used as supports in catalytic processes) using electron-based techniques. In particular, high-resolution scanning tunnelling microscopy can be employed, exploiting the electron tunnelling effect enabled by the extreme thinness of the oxide film.[19-20] However, ultra-thin oxide films exhibit peculiar chemical and physical properties, distinguishing them from their bulk counterparts.[20-23] In particular, magnesium oxide (MgO) has attracted remarkable attention due to its good lattice match with metal supports such as silver (Ag) and molybdenum (Mo), enabling the epitaxial growth of ordered films.[24] Additionally, it was reported that the electron transfer via tunnelling through the MgO film induces the formation of negatively charged, highly reactive sub-nanometric Au particles.[25-26]

Despite the relative structural simplicity of the interface between rock salt MgO and the Ag(100) cubic lattice, numerous papers have shown that the preparation conditions remarkably influence the morphology of the films. For instance, several reports describe the formation of MgO bilayers epitaxially grown on Ag(001),[27] while some of us reported and characterized the formation of extended monolayers.[28] Notably, given the non-negligible oxophilicity of silver,[29] a certain concentration of oxygen is unavoidably trapped at the MgO/Ag interface during the growth process, with relevant impact on the work function of the system and on interfacial charge transfer phenomena. Its optimal concentration was estimated as 25% recurring to ab initio thermodynamics, in good agreement with the value of 30% estimated experimentally at 200 K.[30] However, regions with different loading of interfacial oxygen (O_{int}) can form during the growth process underneath any given MgO island.[31] Such interfacial oxygen can diffuse to the external layer leading to a complete oxidation of the smallest nickel aggregates (in the range of 4-6 atoms) under ultra-high vacuum conditions.[32]

Larger Ni aggregates on MgO/Ag(100) are, on the contrary, mainly metallic.[33] DFT calculations recently performed by some of us showed that such clusters are slightly negatively charged in the absence of O_{int} whereas they assume a slightly positive charge in its presence. This positive charge may increase significantly due to a thermodynamically favourable reverse oxygen spillover phenomenon leading O atoms to diffuse from the MgO/Ag interface through the MgO film and bind to the Ni clusters.[34] This is an important observation, since the oxidation state of Ni particles, often observed for real catalytic systems under operando conditions, strongly influences their chemical reactivity.[35-43]

In the present paper, we shall demonstrate by comparing experimental data with DFT calculations that these Ni nanoclusters (NCs) indeed have an oxidized root and that the

interfacial oxygen concentration determines their spatial distribution at terrace and step sites of the MgO film. These findings are of high importance for the rational design of heterogeneous catalysts, where the strength of the adhesion to the support dictates the activity of the supported particles, and their resistance toward sintering and thermal deactivation.[44]

2. Experimental and theoretical section

Experiments were carried out in an ultrahigh vacuum system hosting a LT-STM (Createc) and connected to a preparation chamber equipped with a Knudsen cell and an O_2 doser for reactive Mg evaporation, a quartz microbalance (QMB) for Mg flux measurements, an e-beam evaporator (Focus EFM 3) mounting a high-purity (99.99%) Ni rod, and with additional facilities for sample cleaning and residual gas analysis.

The Ag(100) substrate is a single crystal cut within 0.1° off the high symmetry plane. Before each experiment, the sample is carefully cleaned by sputtering with Ne^+ ions followed by annealing to a temperature T= 850 K for 5 minutes. Surface cleanliness and order were checked by STM. Monolayer MgO films were grown by reactive deposition at T= 773 K, followed by post-annealing in O_2 atmosphere and slow cooling to T< 450 K.[28] Mg was evaporated from a crucible at T_{ev}=593 K, providing an Mg flux of ∼1 Å/min., in an O_2 pressure $P_{O2}= 1 \times 10^{-6}$ mbar; however, since the oxygen was introduced in the preparation chamber through a doser placed at ∼2 cm from the Ag(100) surface, an effective pressure at least five times higher is expected.[45] Ni was deposited on the MgO/Ag(100) sample at 100 K≤T≤300 K in a background pressure better than 2×10^{-9} mbar. The Ni flux could not be measured during evaporation, so the total Ni coverage is evaluated a posteriori from analysis of STM images, accounting for the different sizes and shapes of the clusters at different deposition temperatures. Samples are cooled to T< 150 K and inserted into the STM immediately after preparation. STM images were recorded at liquid nitrogen temperature with a Pt/Ir tip cut in air under strain and then reshaped by controlled crashes into the surface, so that tunnelling effectively occurs through an Ag tip. The images were acquired in constant current mode, with typical tunnelling currents of ∼ 0.2 nA and bias voltage applied to the sample, −4.0 V≤ V ≤ +4.0 V. The lateral size of the images and the orientation of the surface are determined from atomically resolved measurements of the clean Ag(100) surface (as the one reported in Figure 1f); similarly, heights are calibrated against monatomic Ag steps. STM analysis was performed with the help of WSxM software.[46]

In this study, all first-principles calculations were performed within the framework of spin-polarized DFT [23-24, 47-48] as implemented in the Vienna Ab initio Simulation Package (VASP).[25-27, 49-53] The exchange-correlation potential was parameterized using the Perdew–Burke–Ernzerhof (PBE) [54] functional within the generalized gradient approximation (GGA). The projector-augmented wave (PAW) [55] method was employed to describe the pseudopotentials for O, Mg, Ni, and Ag. A kinetic energy cutoff of $\frac{\hbar^2|k+G|^2}{2m} = 520\ eV$ was employed for the plane-wave basis set, and a vacuum space of ∼20 Å was inserted in the non-periodic direction for all calculations involving clusters on different supports to prevent artificial interactions between neighbouring images. Brillouin zone (BZ) sampling for the relaxation of the MgO(100) monolayer and Ag(100) slab was performed using a Γ-centred

8 × 8 × 1 uniform k-point mesh.[56] For the optimization of NCs on various supports, VASP-Γ was employed with a 1×1×1 k-point grid, suitable for the large supercell sizes. Bader charge analysis was employed to obtain the net charge transfer between the clusters and the supports.[57] During total energy calculations, the electronic relaxation converged to a threshold of 10^{-5} eV between consecutive steps. The optimization of ionic positions and lattice constants was performed until the maximum force on each atom was below 0.01 eV/Å. Furthermore, long-range dispersion effects were considered using the D3 method from Grimme, which includes the Becke-Johnson damping function.[58-59] The magnetic configuration for all calculations was initialized consistently, with a singlet state for Mg, O, and Ag, and a triplet state for Ni, while allowing the configuration to evolve during the self-consistent field iterations. The adsorption energy of the nanoclusters (E_{ads}) can be computed via the following formula

$$E_{ads} = E(Ni_X /Support) – E(Ni_X) – E(Support) \quad (1)$$

where $E(Ni_X /Support)$ represents the total energy of the examined systems, $E(Ni_X)$ and E(Support) denote the total energies of the gas-phase NCs and the support, respectively, and x indicates the number of Ni atoms within the cluster (x=13, 55, 147).

3. Nucleation and migration of Ni Nanoclusters

Figure 1a)-d) shows STM images of Ni NCs grown on monolayer MgO/Ag(100) at four different temperatures: a) 100 K, b) 200 K, c) 250 K and d) 300 K. The protocol followed for the growth of the MgO monolayer is the one reported in ref.[28] leading to extended MgO islands limited only by the size of the Ag terrace underneath. Ni atoms are eventually evaporated by e-beam evaporation. After deposition, they aggregate forming Ni clusters. At 200 K, one-third of the Ni coverage consists of small Ni_xO_y clusters ($4 \leq x \leq 6$) while the rest aggregates into larger, metallic clusters.[33] At 300 K only the larger clusters form. Their apparent average diameter increases thereby from 10-12 Å at 100 K to 17-20 Å at 300 K. A qualitatively similar increase in the Ni/MgO contact area (while the cluster height is conversely reduced) was also noticed by means of Ab-Initio Molecular Dynamics simulations, comparing structures simulated at 0 K and 200 K.[34] Incidentally, dark spots are visible in Figs. 1a. An ultimate assignment on their nature cannot be provided, but we report that changes in contrast within MgO islands were previously attributed to non-uniform distribution of interfacial oxygen, affecting the local density of states of the MgO film.[31]"

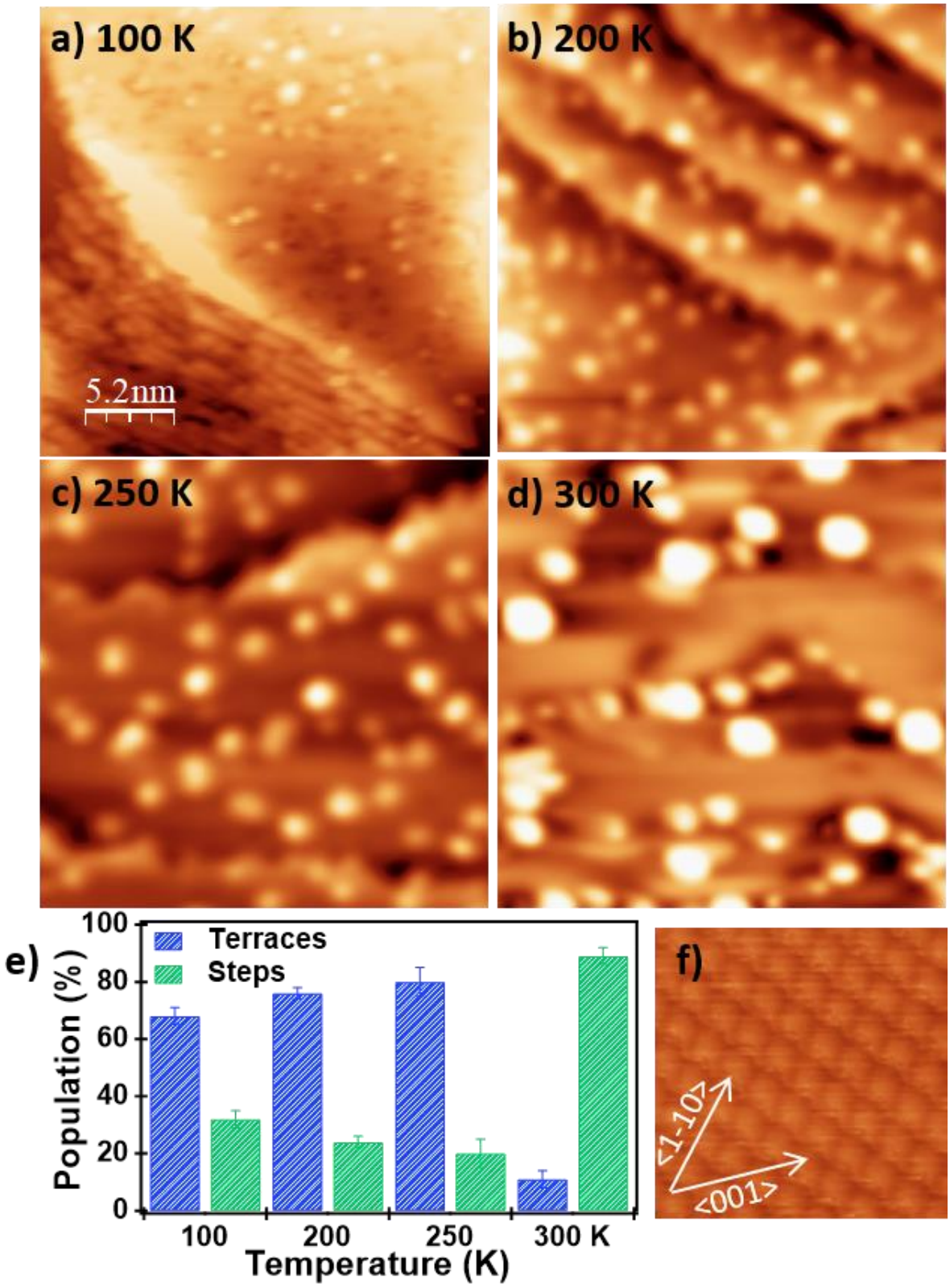


Figure 1. STM images of Ni NCs deposited at different temperatures on monolayer MgO/Ag(100). a) T=100 K, b) T=200 K, c) T=250 K, and d) T=300 K. For all images, size: 26 × 26 nm2; V =+1.0 V. e) Population of clusters at steps and terraces as a function of temperature. The percentages reported in the histogram and in the text are averages over a minimum of several STM images of size (26 × 26) nm^2 (10 images at 100 K, 13 images at 200

K, 5 images at 250 K and 11 images at 300 K). The standard error is reported. f) Atomically resolved image of the clean Ag(100) substrate, from which the high symmetry directions (marked by arrows) and the calibration parameters are deduced.

As evident at a first glance from Fig.1a)-d) and from the histogram of Fig. 1e), the distribution of Ni nanoclusters at MgO steps or terrace sites strongly depends on the deposition temperature: for T≤250 K, they are found mainly at terraces, while at 300 K, they decorate the steps. Indeed, the relative population of NCs at step sites is between 20 and 30% for T≤250 K but it jumps to (89±3) % at 300 K (see Table S1 in Supporting Material).

Formation of metal nanoparticles of larger diameter and the preferential population of clusters at steps with increasing temperature have also been reported for other systems, such as Cu atoms deposited on CeO1.95(111) and Au clusters on NaCl(001).[60-61] This behaviour can be rationalized by considering that, at low T, diffusion is slow and the metal atoms have a high probability of meeting another atom/cluster and aggregating before reaching a step. Although diffusion certainly also plays a role in the present case, the trend in relative population does not show any preferential nucleation at steps below 300 K, even though nanometric clusters grow also at lower temperature. The overviews in Figure a)-c) may appear different, but this is mainly due to the different step density of the imaged MgO areas since statistical analysis over several images (Figure 1e) indicates a similar population of Ni NCs at steps for T≤250 K. Vice versa, the outcome at 300 K suggests the activation of a different mechanism. As it will be discussed in the following, our findings envisage that the presence of interfacial oxygen between MgO and Ag could enhance the clusters stability on terraces. The limited thermal stability of O_{int}, though, may explain the preferential growth at steps at 300 K. We also remark that alternative explanations as the presence of F-centres or OH acting as nucleation centres at the terraces at low temperature can be excluded. On the one hand, oxygen vacancies are unlikely in presence of O_{int}; on the other hand, the presence of OH is ruled out by vibrational spectroscopy analysis performed during CO exposure on Ni NC/MgO/Ag(100) [33].

To gain more insight into this phenomenon, we performed DFT modelling of particles of comparable size to those observed in the STM measurements. First, we note that the measured cluster diameter should be corrected for convolution with the STM tip, so that a size in the range of 5 nm to 15 nm can be inferred. Given the highly complex polymorphism and the actual composition of supported metal clusters within the observed size range, we decided to focus on specific clusters exhibiting high stability in the gas phase. Therefore, we chose the icosahedral Ni_{13}, Ni_{55} and Ni_{147} clusters, corresponding to the "magic numbers" for which the nanoparticles exhibit complete outer atomic shells and compact structures.[62] It must be stated, however, that other geometries could as well be possible, and an exhaustive study of the polymorphism in supported particles is beyond the scope of the present work.

As shown in Fig. S1 of the Supporting Material, they are all characterized by triangular closed packed nanofacets; in the gas phase their diameter spans from 4.67 Å (Ni_{13}), to 9.24 Å (Ni_{55}), and to 13.93 Å (Ni_{147}) (see Table 1).

The adsorption of these clusters was simulated on the various MgO supports on Ag(100) schematized in Fig. S2: a continuous MgO monolayer (ML_c, panel a), a finite monolayer

MgO island (ML_i, panel b), a continuous MgO bilayer (BL_c, panel c), and a stepped MgO BL (BL_s, panel d).

The results of the simulations are reported in Table 1. The side views of the corresponding relaxed structures are shown in Fig. 2. First, one can notice that the icosahedral clusters maintain a quasi-spherical geometrical arrangement on all MgO supports: their height with respect to the surface (measured as the difference in the z coordinate between the apical Ni atom of the cluster and the basal MgO plane) and their diameter display very similar values (Table 1, col. III and IV). On ML_i, the clusters sit at the edge of the MgO island, in contact with the bare Ag. In this case, Ni55 and Ni147 clusters retain their quasi-spherical shape, while the Ni13 ones wet the bare metal. We remark that, in general, the calculated physical heights exceed the values previously reported in ref. [33]; however, the latter ones correspond to the apparent height measured by STM, so that a direct comparison is misleading. The clusters' magnetization (Table 1, col. V) does not undergo drastic changes relative to the gas-phase, with a general small increase (Ni_{13}) or small decrease (Ni_{55} and Ni_{147}). Ni_{13} maintains an almost neutral charge state upon adsorption on the various MgO supports featured in Figure 2. At the same time, Ni_{55} and Ni_{147} acquire a sizable negative charge, with little difference on MLs or BLs (col. VI). Interestingly, the interfacial dipole (col. VII) does not correlate with such a charge transfer: if negative charge is injected into a metal cluster adsorbed on the surface, a positive dipole moment would be expected; however, neither its sign nor its intensity shows a regular trend. This could be explained by an internal compensation effect among the dipole moment generated at the MgO/Ag interface, the contribution of charge transfer to the adsorbed Ni cluster, and charge redistribution phenomena within the metal particle.

Table 1. Ni_X (X=13, 55, 147) adsorbed on a continuous MgO ML/Ag (ML_c), an MgO ML island on Ag (ML_i), a continuous MgO BL/Ag (BL_c), and a stepped MgO BL/Ag (BL_s). Columns III to VIII refer, respectively, to cluster height with respect to the basal plane (h, Å), cluster diameter (d, Å), magnetization (μ, μ_B), Bader charge (Q, |e|), interfacial dipole moment (dip, |e|× Å), and adsorption energy (E_{ads}, eV).

I Support	II Ni_x	III h (Å)	IV d (Å)	V μ (μ_B)	VI Q (|e|)	VII dip (|e|× Å)	VIII E_{ads} (eV)
Gas-phase	13	-	4.67	8.00	-	-	-
	55	-	9.24	39.94	-	-	-
	147	-	13.93	99.19	-	-	-
ML_c	13	5.68	4.80	8.97	-0.11	-3.46	-5.39
	55	9.38	9.23	36.63	-0.89	-1.50	-8.46
	147	13.42	13.95	96.58	-1.47	+0.03	-12.12
ML_i	13	3.62	4.79	8.67	-0.02	-1.32	-5.10
	55	9.39	9.29	37.87	-0.67	+0.03	-7.25
	147	13.66	13.96	96.51	-1.07	+0.87	-9.65
BL_c	13	5.94	4.78	8.35	-0.27	-4.51	-5.14
	55	9.98	9.32	36.78	-1.63	-1.80	-7.78
	147	13.74	13.97	95.32	-2.55	+0.07	-11.37
BL_s	13	5.53	5.65	9.45	+0.10	-3.77	-8.22
	55	10.21	9.62	37.01	-1.30	-1.75	-9.71
	147	13.61	13.96	95.03	-2.22	-0.04	-15.39

Notably, a clear trend in the adsorption energy emerges for clusters of all sizes (Table 1, col. VIII): the strongest adhesion (corresponding to the most negative values of E_{ads}) is observed on the stepped BL, followed by the continuous ML, the continuous BL, and the stepped ML. This clearly shows the strong action as trapping sites exerted by the MgO steps. The stronger adhesion on continuous MLs compared to continuous BLs could be ascribed to two factors: i)

a stabilizing hybridization of the electron densities of the Ni atoms with the silver atoms, enabled by the extreme thinness of the MgO film, and ii) the larger work function of the continuous MgO ML/Ag compared to MgO BL/Ag, which could affect the charge injection to the Ni particle, strengthening the bond. The stronger binding of metal species on ML compared to BL has been previously observed for single atoms.[63] Finally, it is worth noting that the MgO ML/Ag interface is not an efficient trapping site. Indeed, all the clusters show the lowest E_{ads} on the ML_i substrate. Probably the stronger bonding between the truncated ML borders and the Ag substrate reduces site reactivity with respect to the stepped BL. We remark, however, that the BL_s model best reproduces our experimental conditions at step sites, where a monolayer MgO film covers both the top and the bottom terraces at the steps, with no Ag exposed.

Therefore, our calculations predict that the model of Fig. 2d is the most stable among the investigated ones, and Ni clusters are expected to decorate MgO steps. However, this result contrasts with the experimental data, showing a significant population of terraces at T≤250 K. The failure of the model in reproducing the experimental results indicates that an important parameter has been overlooked. Considering the role of interfacial oxygen in the growth of ordered MgO monolayers and in the spontaneous oxidation of ultrasmall Ni clusters, we focused our attention on the presence of O_{int}, and we included it in the calculations.[28-32]

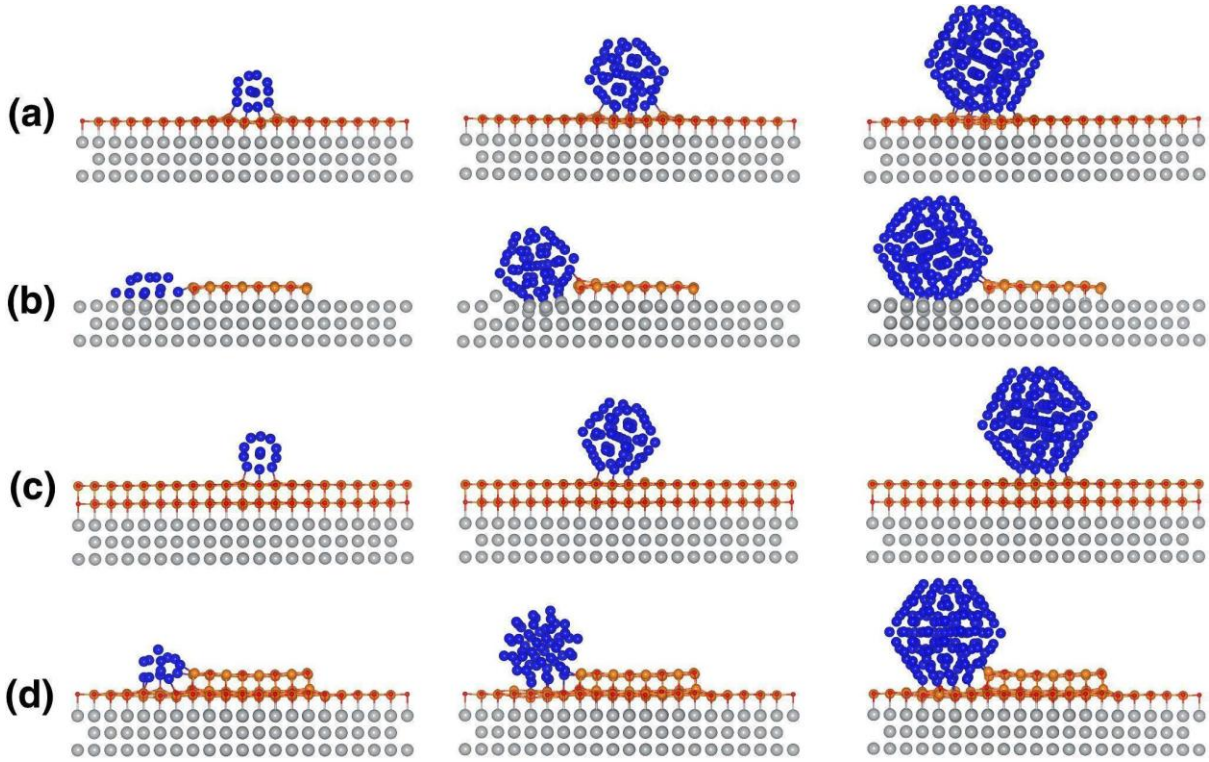


Figure 2. Side views of the calculated structures of Ni clusters on a) ML_c, b) ML_i, c) BL_c, d) BL_s.

4. Effect of the interfacial oxygen and clusters oxidation

The effect of adding oxygen at the interface in the computational models is shown in Fig.3 and Table 2 for the three most interesting cases previously described: continuous ML (ML_c_O), continuous BL (BL_c_O), and stepped BL (BL_s_O). In the models we assume 25% coverage of interfacial oxygen, corresponding to the optimal concentration reported in our previous work.[30] Partial oxidation of the Ni atoms in contact with the MgO film occurs, leading to global stabilization of the clusters, an effect that is more pronounced for the smallest nanoparticles. The observed clusters are indeed compatible with the presence of an oxide root as shown in the Supporting Material (Fig. S3).

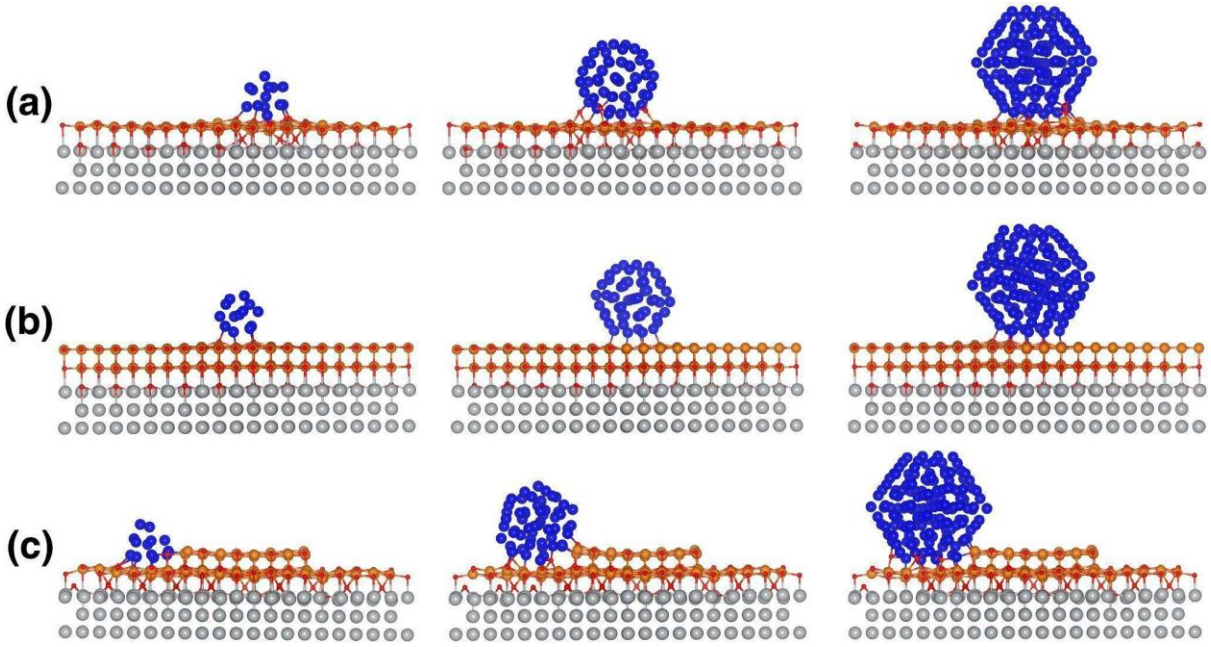


Figure 3. Side views of the calculated structures of Ni clusters on a) ML_c_O, b) BL_c_O, c) BL_s_O.

The data in Table 2 highlight the strong effect of O_{int} on the MgO surface physical and chemical properties and on the MgO interaction with Ni clusters. In particular, the main structural parameters of the adsorbed Ni_X are only marginally affected: comparing Table 1 and Table 2 one can notice only a negligible or small decrease in the physical height of the clusters (col. III). Vice versa, relevant changes are observed in the electronic and magnetic properties, as well as the adhesion strength and relative stability on the various supports. In general, the magnetization of Ni_X (col. V) is significantly larger on supports bearing 25% O_{int}, in particular on ML_c_O and BL_s_O. For the continuous MgO bilayer (BL_c_O), the effect is less pronounced. The change in the magnetization is related to an inversion of the charge state of the supported clusters that display negative charge on ML_c and BL_s (Table 1, col. VI) and positive (and generally larger) charge on ML_c_O and BL_s_O (Table 2, col. VI), in agreement

with previous findings by some of us.[34] Interestingly, the effect is much smaller on BL_c_O, where the charge of the supported Ni clusters is negative (though less negative than in the absence of O_{int}, Table 1) or almost neutral. Steps, thus, represent an intermediate case between ML terraces, where the stabilization exerted by O_{int} on metal clusters is very strong, and BL terraces, where the effect is very weak.

In general, in the presence of interfacial oxygen, the adsorption energy is remarkably larger on all types of MgO supports (Table 2, col. VIII). However, this enhancement in stability is much stronger in ML_c_O than in MgO bilayers and it affects the overall stability trend. Indeed, in the presence of interfacial oxygen, the clusters are bound more strongly on continuous ML terraces (ML_c_O) than at bilayer steps (BL_s_O) and this behaviour is opposite to the one predicted in the absence of Oint (compare ML_c and BL_s in Table 1, col. VIII).

The different effect of an analogous concentration of interfacial oxygen on MgO MLs and BLs can be attributed to the different thickness of the insulating MgO layers. As expected, the effect of O_{int} is smaller on thicker BLs compared to MLs.~~ultimate thickness limit of the insulating MgO layer separating the adsorbed Ni clusters from the Ag support.~~

Table 2. Ni_X (X=13, 55, 147) adsorbed on MgO/O/Ag (bearing 25% O_{int} at the MgO/Ag interface). Calculated values for the continuous MgO ML/O/Ag (ML_c_O), continuous MgO BL/O/Ag (BL_c_O), and stepped BL/O/Ag (BL_s_O) supports are reported. Columns III to VIII refer, respectively, to cluster height with respect to the basal plane (h, Å), cluster diameter (d, Å), cluster magnetization (μ, μ_B), Bader charge (Q, |e|), interfacial dipole moment (dip, |e|× Å), and adsorption energy (E_{ads}, eV).

I Support	II Ni_x	III h (Å)	IV d (Å)	V μ (μ_B)	VI Q (|e|)	VII dip (|e|× Å)	VIII E_{ads} (eV)
ML_c_O	13	5.47	4.77	10.69	+0.91	-1.42	-23.36
	55	9.12	9.27	40.14	+1.78	-0.57	-28.77
	147	13.20	13.96	100.14	+1.92	+0.55	-32.65
BL_c_O	13	6.02	4.86	9.58	+0.48	-2.08	-8.22
	55	9.79	9.31	37.96	-0.08	-0.62	-7.95
	147	13.66	14.02	97.86	-0.02	+0.32	-11.91
BL_s_O	13	5.63	6.15	11.79	+1.41	-0.52	-15.53
	55	10.17	9.67	38.93	+1.33	+0.19	-17.28
	147	11.52	14.42	97.29	+1.91	+0.87	-23.12

We can now explain the effect of deposition temperature on the cluster distribution observed in the STM experiments using these DFT results. Firstly, we recall that Ni clusters on monolayer MgO terraces are best modelled by Ni_X adsorption at the ML_c or ML_c_O supports, whereas BL_s or BL_s_O are more suitable for representing cluster adsorption at the MgO steps. DFT clearly indicates the essential role of interface oxygen concentration and of its temperature dependence. Indeed, ~~the uniform distribution of clusters observed experimentally at 100 K suggests that Ni adatoms have enough kinetic energy to diffuse on the surface at any temperature considered here~~ the presence of aggregations larger than few-atoms at 100 K already, in agreement with previous reports [33], is a key-point in indicating the presence of a mechanism acting beyond bare thermally enhanced diffusion. On the other hand, theory predicts that, in the absence of interfacial oxygen, the Ni clusters are most stably adsorbed at MgO steps of the BL_s supports. In contrast, in the presence of O_{int}, partial oxidation and adsorption on ML terraces (ML_c_O) is favoured.

Therefore, we can rationalize the different spatial distribution of Ni clusters vs growth temperature considering that for T≤250 K there is enough interfacial oxygen for the clusters to get partially oxidized and anchor at terraces; vice versa, at T=300 K the O_{int} concentration is depleted and MgO steps become the most favourable adsorption site.

This picture is supported by the calculation of the O_{int} free energy at $P=1 \times 10^{-9}$ mbar and T=100-400 K (see Table S2 in the Supporting Material), i.e. in conditions close to the experimental ones for Ni clusters growth. At 25% O_{int} coverage, Ni NCs are stable on all supports, with a trend in binding energy that is ML_c ≈ BL_c > BL_s. However, the adsorption energy values decrease with increasing temperature, becoming almost negligible at 400 K. Experimentally, an estimate of O_{int} is available only at 200 K but, considering that comparison with DFT calculations are only qualitative, it is reasonable to suppose that the stability of O_{int} is negligible already at RT.[28] It is also interesting, in this respect, to mention that the different O_{int} stability in ML_c and BL_c (i.e. in the central region of MgO islands) compared to steps could induce oxygen diffusion within the MgO/Ag interface. Overall, the ~~The~~ Oint concentration can vary due to various factors; direct evaporation of oxygen is unlikely under the observed experimental conditions but reverse oxygen spillover or diffusion into the subsurface Ag(100) region must be considered. Reverse oxygen spillover from the MgO/Ag interface to the external surfaces of the adsorbed Ni clusters was recently proved to be strongly thermodynamically favoured for Ni_{55} clusters by DFT calculations. It implies a concerted mechanism in which O atoms from the MgO lattice move to the Ni cluster borders and the oxygen vacancies are refilled by interfacial oxygen species.[34] It was not possible, though, to evaluate the actual diffusion barrier for this process. From the experimental point of view, the deposition of Ni adatoms takes place in ultrahigh vacuum so that O_{int} is the only oxygen reservoir available for the observed formation of NiO_x clusters.[32] It is thus possible that, in the initial stage of nucleation and growth of the clusters, concomitant partial oxidation takes place, as also supported by the analysis of the shapes and height profiles in the STM images reported in the Supporting Material, and the occasional identification of the previously described Ni_xO_y oligomers.[32] At higher temperatures, the kinetic barriers hindering this mechanism will be more easily overcome. This effect, combined with the higher mobility of deposited Ni atoms, contributes to explaining the change in the clusters' size and spatial

distribution observed at room temperature. The diffusion of partially oxidized Ni_xO_y entities could, in principle, also contribute to further non-trivial growth mechanisms.

The diffusion of the interfacial oxygen back into the Ag subsurface is difficult to monitor experimentally. Some of us demonstrated, using photoelectron spectroscopy, that a subsurface oxygen species migrates into the bulk at T > 280 K on O/Ag(210).[64] However, the situation is different if oxygen is trapped at the MgO/Ag interface, so that we must rely on DFT calculations showing that diffusion into the Ag bulk is thermodynamically unfavourable (see Supporting Maerial, Fig. S4). The most probable fate of the subsurface oxygen is therefore its migration into the larger Ni clusters forming at RT.

Finally, we remark that the diffusion barrier for such clusters is expected to be around 1/3 of their adsorption energy, which implies that they should not sinter at temperatures lower than 600 K. This agrees well with the size distribution of the grown nanoparticles, having a diameter between 1.0 and 1.5 nm, i.e. compatible with the size of Ni_{55} and Ni_{147}, and demonstrates the active role of a suitable substrate in the optimization of catalytic materials.[33] This result is potentially quite appealing to obtain nanoparticles of kinetically limited shape under temperature conditions which are considered the optimal ones for CO_2 methanation on non-reducible oxide supports (640 K according to ref. [10]). It must be stated, though, that the catalytic operating conditions do not envisage only high temperature, but also exposure to high pressure of reactive gases such as oxygen, hydrogen, CO_2 and others. Our previous computational work [34] assesses the stability of supported Ni clusters in an oxidizing environment, but their behaviour under reducing conditions and exposure to reactive gases remains to be investigated.

5. Conclusions

In this study we show that the nucleation, spatial distribution and thermal stability of Ni nanoclusters on MgO/Ag(100) surfaces are strongly influenced by the morphology of the substrate by using STM analysis and DFT calculations.

The MgO/Ag interface acts as a reservoir releasing O in oxygen poor conditions or segregating it under oxygen rich conditions. The observed nucleation pattern highlights the combined role of interfacial oxygen and diffusion kinetics in directing cluster growth. Furthermore, stability analysis reveals that Ni clusters retain their structural integrity within a definite size regime, while the migration to steps observed at 300 K could further lead to agglomeration. These results provide fundamental insights into metal oxide/interface behaviour and open pathways for tailoring Ni NCs for catalysis and nanoscale devices.

Acknowledgements

We thank Jagriti Pal for participating in the initial stages of STM experiments.

We acknowledge funding from the European Union – NextGenerationEU, Mission 4, Component 1, through the Italian Ministry of University and Research under projects PRIN-

PNRR P20227XSAH, CUP B53D23028390001 and project PRIN 2022 2022LS74H2, CUP B53D23013810006.

Computational support from CINECA supercomputing centre is kindly acknowledged.

Author Contributions. Conceptualization: S.T., M.R. L.S.; methodology and formal analysis: A.S. L.S., M.J.V., S.T.; investigation: all authors; Funding acquisition: S.T., L.S., M.R.; data curation: A.S. L.S., M.J.V., S.T.; writing—original draft preparation: A.S. L.S., M.J.V., S.T, M.R., writing—review and editing: all authors. All authors have read and agreed to the published version of the manuscript.

Conflicts of Interest: The authors declare no conflicts of interest.

References

[1] M. Monai, M. Gambino, S. Wannakao, B.M. Weckhuysen, Propane to olefins tandem catalysis: a selective route towards light olefins production, Chemical Society Reviews 50(20) (2021) 11503-11529.

[2] J. Gong, R. Luque, Catalysis for production of renewable energy, Chemical Society Reviews 43(22) (2014) 7466-7468.

[3] J.R. Lockemeyer, T.L. Lohr, M.A. Reynolds, A. van der Made, Catalysis for the Energy Transition, ChemCatChem (2025) e00588.

[4] G. Centi, J. Čejka, Needs and gaps for catalysis in addressing transitions in chemistry and energy from a sustainability perspective, ChemSusChem 12(3) (2019) 621-632.

[5] I. Chorkendorff, J.W. Niemantsverdriet, Concepts of modern catalysis and kinetics, John Wiley & Sons, 2017.

[6] Y. Xia, H. Yang, C.T. Campbell, Nanoparticles for catalysis, ACS Publications, (2013), pp. 1671-1672.

[7] D. Astruc, Introduction: nanoparticles in catalysis, ACS Publications, 2020, pp. 461-463.

[8] U. Heiz, E.L. Bullock, Fundamental aspects of catalysis on supported metal clusters, Journal of Materials Chemistry 14(4) (2004) 564-577.

[9] E. Bus, R. Prins, J.A. van Bokhoven, Origin of the cluster-size effect in the hydrogenation of cinnamaldehyde over supported Au catalysts, Catalysis Communications 8(9) (2007) 1397-1402.

[10] E.B. Sterk, A.-E. Nieuwelink, M. Monai, J.N. Louwen, E.T. Vogt, I.A. Filot, B.M. Weckhuysen, Structure sensitivity of CO2 conversion over nickel metal nanoparticles explained by micro-kinetics simulations, JACS Au 2(12) (2022) 2714-2730.

[11] O. Dulub, W. Hebenstreit, U. Diebold, Imaging cluster surfaces with atomic resolution: the strong metal-support interaction state of Pt supported on TiO_2(110), Physical Review Letters 84(16) (2000) 3646.

[12] S. Tauster, Strong metal-support interactions, Accounts of Chemical Research 20(11) (1987) 389-394.

[13] Z.-H. Qin, M. Lewandowski, Y.-N. Sun, S. Shaikhutdinov, H.-J. Freund, Morphology and CO adsorption on platinum supported on thin Fe3O4(111) films, Journal of Physics: Condensed Matter 21(13) (2009) 134019.

[14] M. Lewandowski, Y.-N. Sun, Z.-H. Qin, S. Shaikhutdinov, H.-J. Freund, Promotional effect of metal encapsulation on reactivity of iron oxide supported Pt catalysts, Applied Catalysis A: General 391(1-2) (2011) 407-410.

[15] J.Y. Park, L.R. Baker, G.A. Somorjai, Role of hot electrons and metal–oxide interfaces in surface chemistry and catalytic reactions, Chemical Reviews 115(8) (2015) 2781-2817.

[16] T. Lunkenbein, J. Schumann, M. Behrens, R. Schlögl, M.G. Willinger, Formation of a ZnO overlayer in industrial Cu/ZnO/Al2O3 catalysts induced by strong metal–support interactions, Angewandte Chemie 127(15) (2015) 4627-4631.

[17] F. Polo-Garzon, T.F. Blum, Z. Bao, K. Wang, V. Fung, Z. Huang, E.E. Bickel, D.-e. Jiang, M. Chi, Z. Wu, In situ strong metal–support interaction (SMSI) affects catalytic alcohol conversion, ACS Catalysis 11(4) (2021) 1938-1945.

[18] J.A. Farmer, C.T. Campbell, Ceria maintains smaller metal catalyst particles by strong metal-support bonding, Science 329(5994) (2010) 933-936.

[19] T. Zambelli, J. Wintterlin, J. Trost, G. Ertl, Identification of the" active sites" of a surface-catalyzed reaction, Science 273(5282) (1996) 1688-1690.

[20] N. Nilius, Properties of oxide thin films and their adsorption behavior studied by scanning tunneling microscopy and conductance spectroscopy, Surface Science Reports 64(12) (2009) 595-659.

[21] S. Street, C. Xu, D. Goodman, The physical and chemical properties of ultrathin oxide films, Annual Review of Physical Chemistry 48(1) (1997) 43-68.

[22] J.M. Rondinelli, N.A. Spaldin, Structure and properties of functional oxide thin films: insights from electronic-structure calculations, Advanced Materials 23(30) (2011) 3363-3381.

[23] L. Giordano, G. Pacchioni, Oxide films at the nanoscale: new structures, new functions, and new materials, Accounts of Chemical Research 44(11) (2011) 1244-1252.

[24] G. Pacchioni, H. Freund, Electron transfer at oxide surfaces. The MgO paradigm: from defects to ultrathin films, Chemical Reviews 113(6) (2013) 4035-4072.

[25] D. Ricci, A. Bongiorno, G. Pacchioni, U. Landman, Bonding Trends and Dimensionality Crossover of Gold Nanoclusters on Metal-Supported MgO Thin Films, Physical Review Letters 97(3) (2006) 036106.

[26] F. Calaza, C. Stiehler, Y. Fujimori, M. Sterrer, S. Beeg, M. Ruiz-Oses, N. Nilius, M. Heyde, T. Parviainen, K. Honkala, Carbon dioxide activation and reaction induced by electron transfer at an oxide–metal interface, Angewandte Chemie International Edition 54(42) (2015) 12484-12487.

[27] E. Carrasco, M.A. Brown, M. Sterrer, H.-J. Freund, K. Kwapien, M. Sierka, J. Sauer, Thickness-dependent hydroxylation of MgO(001) thin films, The Journal of Physical Chemistry C 114(42) (2010) 18207-18214.

[28] J. Pal, M. Smerieri, E. Celasco, L. Savio, L. Vattuone, M. Rocca, Morphology of monolayer MgO films on Ag (100): switching from corrugated islands to extended flat terraces, Physical Review Letters 112(12) (2014) 126102.

[29] N. Janulaitis, C.T. Campbell, Predicting Adhesion Energies of Late Transition Metal Nanoparticles to Oxide Support Surfaces Using Oxide Reducibility and Metal Oxophilicity: Toward Predicting Catalyst Performance, ACS Catalysis 15(9) (2025) 6874-6880.

[30] J. Pal, M. Smerieri, E. Celasco, L. Savio, L. Vattuone, R. Ferrando, S. Tosoni, L. Giordano, G. Pacchioni, M. Rocca, How growing conditions and interfacial oxygen affect the final morphology of MgO/Ag(100) films, The Journal of Physical Chemistry C 118(45) (2014) 26091-26102.

[31] L. Savio, M. Smerieri, L. Vattuone, S. Tosoni, G. Pacchioni, M. Rocca, Interface Oxygen Induced Internal Structures of Ultrathin MgO Islands Grown on Ag(100), The Journal of Physical Chemistry C 124(16) (2020) 8834-8842.

[32] M. Smerieri, J. Pal, L. Savio, L. Vattuone, R. Ferrando, S. Tosoni, L. Giordano, G. Pacchioni, M. Rocca, Spontaneous oxidation of Ni nanoclusters on MgO monolayers induced by segregation of interfacial oxygen, The Journal of Physical Chemistry Letters 6(15) (2015) 3104-3109.

[33] L. Savio, M. Smerieri, J. Pal, E. Celasco, M. Rocca, L. Vattuone, 2D Ni Nanoclusters on Ultrathin MgO/Ag(100), The Journal of Physical Chemistry C 124(1) (2019) 482-488.

[34] M. Jahangirzadeh Varjovi, S. Tosoni, DFT Investigation of X55 (X= Ni, Pd, and Pt) Clusters on Ultrathin Supported MgO Films: Evidence of Oxygen Spillover and Relevance for Catalytic Model Studies, The Journal of Physical Chemistry C 128(50) (2024) 21331-21342.

[35] W. Gac, T. Borowiecki, P. Kowalik, Nickel Nanocatalysts for Methane Steam Reforming, Nanotechnology in Catalysis: Applications in the Chemical Industry, Energy Development, and Environment Protection (2017) 401-420.

[36] A. Parmaliana, F. Arena, F. Frusteri, S. Coluccia, L. Marchese, G. Martra, A. Chuvilin, Magnesia-supported nickel catalysts: II. Surface properties and reactivity in methane steam reforming, Journal of Catalysis 141(1) (1993) 34-47.

[37] S. Schauermann, N. Nilius, S. Shaikhutdinov, H.-J. Freund, Nanoparticles for heterogeneous catalysis: new mechanistic insights, Accounts of Chemical Research 46(8) (2013) 1673-1681.

[38] A. Cadi-Essadek, A. Roldan, X. Aparicio-Anglès, N.H. De Leeuw, CO_2 and H_2 adsorption and reaction at Nin/YSZ(111) interfaces: a density functional theory study, The Journal of Physical Chemistry C 122(34) (2018) 19463-19472.

[39] G.I. Siakavelas, N.D. Charisiou, S. AlKhoori, A.A. AlKhoori, V. Sebastian, S.J. Hinder, M.A. Baker, I. Yentekakis, K. Polychronopoulou, M.A. Goula, Highly selective and stable nickel catalysts supported on ceria promoted with Sm_2O_3, Pr_2O_3 and MgO for the CO_2 methanation reaction, Applied Catalysis B: Environmental 282 (2021) 119562.

[40] C.R. Rêgo, P. Tereshchuk, L.N. Oliveira, J.L. Da Silva, Graphene-supported small transition-metal clusters: A density functional theory investigation within van der Waals corrections, Physical Review B 95(23) (2017) 235422.

[41] W.-S. Dong, K.-W. Jun, H.-S. Roh, Z.-W. Liu, S.-E. Park, Comparative study on partial oxidation of methane over Ni/ZrO_2, Ni/CeO_2 and Ni/Ce–ZrO_2 catalysts, Catalysis Letters 78(1) (2002) 215-222.

[42] A. Caballero, J.P. Holgado, V.M. Gonzalez-delaCruz, S.E. Habas, T. Herranz, M. Salmeron, In situ spectroscopic detection of SMSI effect in a Ni/CeO_2 system: hydrogen-induced burial and dig out of metallic nickel, Chemical Communications 46(7) (2010) 1097-1099.

[43] G.G. Asara, L.O. Paz-Borbón, F. Baletto, "Get in Touch and Keep in Contact": Interface effect on the oxygen reduction reaction (ORR) activity for supported PtNi nanoparticles, ACS Catalysis 6(7) (2016) 4388-4393.

[44] C.T. Campbell, The energetics of supported metal nanoparticles: relationships to sintering rates and catalytic activity, Accounts of Chemical Research 46(8) (2013) 1712-1719.

[45] F.C. Henn, M.E. Bussell, C.T. Campbell, A simple means for reproducibly dosing low vapor pressure and/or reactive gases to surfaces in ultrahigh vacuum, Journal of Vacuum Science & Technology A: Vacuum, Surfaces, and Films 9(1) (1991) 10-13.

[46] I. Horcas, R. Fernández, J. Gomez-Rodriguez, J. Colchero, J. Gómez-Herrero, A.M. Baro, WSXM: A software for scanning probe microscopy and a tool for nanotechnology, Review of Scientific Instruments 78(1) (2007).

[47] W. Kohn, L.J. Sham, Self-consistent equations including exchange and correlation effects, Physical Review 140(4A) (1965) A1133.

[48] P. Hohenberg, W. Kohn, Density functional theory (DFT), Phys. Rev 136(1964) (1964) B864.

[49] S. Schintke, S. Messerli, M. Pivetta, F. Patthey, L. Libioulle, M. Stengel, A. De Vita, W.-D. Schneider, Insulator at the ultrathin limit: MgO on Ag (001), Physical Review Letters 87(27) (2001) 276801.

[50] G. Kresse, J. Hafner, Ab initio molecular dynamics for liquid metals, Physical Review B 47(1) (1993) 558.

[51] G. Kresse, J. Hafner, Ab initio molecular-dynamics simulation of the liquid-metal–amorphous-semiconductor transition in germanium, Physical Review B 49(20) (1994) 14251.

[52] G. Kresse, J. Furthmüller, Efficiency of ab-initio total energy calculations for metals and semiconductors using a plane-wave basis set, Computational Materials Science 6(1) (1996) 15-50.

[53] G. Kresse, J. Furthmüller, Efficient iterative schemes for ab initio total-energy calculations using a plane-wave basis set, Physical Review B 54(16) (1996) 11169.

[54] J.P. Perdew, K. Burke, M. Ernzerhof, Generalized gradient approximation made simple, Physical Review Letters 77(18) (1996) 3865.

[55] P.E. Blöchl, Projector augmented-wave method, Physical review B 50(24) (1994) 17953.

[56] H.J. Monkhorst, J.D. Pack, Special points for Brillouin-zone integrations, Physical Review B 13(12) (1976) 5188.

[57] G. Henkelman, A. Arnaldsson, H. Jónsson, A fast and robust algorithm for Bader decomposition of charge density, Computational Materials Science 36(3) (2006) 354-360.

[58] S. Grimme, S. Ehrlich, L. Goerigk, Effect of the damping function in dispersion corrected density functional theory, Journal of Computational Chemistry 32(7) (2011) 1456-1465.

[59] S. Grimme, J. Antony, S. Ehrlich, H. Krieg, A consistent and accurate ab initio parametrization of density functional dispersion correction (DFT-D) for the 94 elements H-Pu, The Journal of Chemical Physics 132(15) (2010).

[60] T.E. James, S.L. Hemmingson, C.T. Campbell, Energy of supported metal catalysts: from single atoms to large metal nanoparticles, ACS Catalysis 5(10) (2015) 5673-5678.

[61] T. Hynninen, G. Cabailh, A.S. Foster, C. Barth, Defect mediated manipulation of nanoclusters on an insulator, Scientific Reports 3(1) (2013) 1270.

[62] T. Rapps, R. Ahlrichs, E. Waldt, M.M. Kappes, D. Schooss, On the structures of 55-atom transition-metal clusters and their relationship to the crystalline bulk, Angewandte Chemie International Edition 52(23) (2013).

[63] S. Tosoni, G. Pacchioni, Bonding Properties of Isolated Metal Atoms on Two-Dimensional Oxides, The Journal of Physical Chemistry C 124(38) (2020) 20960-20973.

[64] L. Savio, A. Gerbi, L. Vattuone, A. Baraldi, G. Comelli, M. Rocca, Monitoring super-and subsurface oxygen on Ag (210) by high energy resolution X-ray photoelectron spectroscopy: Subsurface diffusion and segregation, The Journal of Physical Chemistry B 110(2) (2006) 942-947.

Declaration of interests

☒The authors declare that they have no known competing financial interests or personal relationships that could have appeared to influence the work reported in this paper.

☐The authors declare the following financial interests/personal relationships which may be considered as potential competing interests:

Manuscript Number: SURFIN-D-26-05175

The role of interfacial oxygen in the nucleation and stability of Ni Nanoclusters at MgO ultrathin films: Insights from STM and first-principles DFT calculations

Dear Dr. Baibarac,

Thank you for reviewing our manuscript. We are glad to see that both reviewers, albeit requiring relevant changes, considered our work as potentially suitable for publication on Surfaces and Interfaces.

We are grateful to both reviewers for their insightful and constructive comments, which we took in most serious consideration while revising the manuscript. We also carefully revised the manuscript to fix typos and minor inconsistencies.

Attached please find the revised version of our work, which we hope will be suitable for publication. A point-to-point reply to all comments from reviewers, and all related changes in the manuscript, is enclosed to this letter.

I am looking forward to hearing from you.

Best regards

Sergio Tosoni (on behalf of all authors)

Reviewer #1: SURFIN-D-26-05175

The authors present a combined experimental scanning tunnelling microscopy and first-principles calculations study of the nucleation and spatial distribution of Ni nanoclusters grown by deposition of Ni atoms on MgO monolayer films supported on Ag(100) at temperature between 100 K and 300 K.

The manuscript presents interesting results and may be suitable for publication in Surface and Interfaces. Nevertheless, the authors should address the following questions and comments before the manuscript can be considered for publication.

Authors reply: We are grateful to the Reviewer for their insightful comments and their positive evaluation on the suitability of our manuscript.

Minor Editorial Corrections

1) Punctuation error in the Abstract: The text reads: "...different spatial distribution with deposition temperature At and below 250 K...". A period is missing after "temperature", or alternatively, the word "At" should begin with a lowercase letter if it is intended to be part of the same sentence.

Authors reply: We fixed this error, thank you.

2) A reference in the text is placed before the final punctuation mark in a sentence.

Authors reply: We checked the correct placement of the references throughout the text.

3) Inconsistency in table citations: The main text refers to "Table I" (pg 8), whereas the actual table inserted in the manuscript is labeled "Table 1". This discrepancy appears in several parts of the manuscript.

Authors reply: Thank you for spotting this discrepancy, it has been fixed.

4*) Incomplete or grammatically incorrect sentence: In Section 4 (pg 12), there is a sentence that appears to have lost words during editing: "The different effect of an analogous concentration of interfacial oxygen on MgO MLs and BLs can ultimate thickness limit of the insulating MgO layer...". The authors probably intended to write something like "can be attributed to the ultimate thickness limit" or a similar expression.*

Authors reply: In compliance with this remark, we rephrased the mentioned paragraph as follows:

"The different effect of an analogous concentration of interfacial oxygen on MgO MLs and BLs can be attributed to the different thickness of the insulating MgO layers. As expected, the effect of O_{int} is smaller on thicker BLs compared to MLs.~~ultimate thickness limit of the insulating MgO layer separating the adsorbed Ni clusters from the Ag support.~~"

5) Missing reference: At the end of Section 4, the text states: "...(640 K according to ref).". The reference number has been omitted from the parenthetical citation.

Authors reply: We fixed this format error, by changing "ref).[10]" into "ref.[10])."

6) *Redundant punctuation in the Experimental Section: There is a comma immediately following the period of an abbreviation: "...Mg flux of ~1 Å/min.,. in an O_2 pressure...".*

Authors reply: We fixed this, thank you.

7) Inconsistency in capitalization: The title uses "Ni Nanoclusters" (with a capital "N"), whereas the keywords and the rest of the text frequently use "Ni nanoclusters". It is recommended to standardize the capitalization of this technical term throughout the manuscript.

Authors reply: We standardised the capitalization through the text, thank you.

Specific Comments

8) Direct experimental evidence of Oint depletion: The manuscript attributes the shift of Ni clusters to step sites at 300 K to the depletion of interfacial oxygen (Oint), supported primarily by DFT and free energy calculations. However, the authors state that experimental estimates of Oint are only available at 200 K. Can you provide direct experimental evidence (e.g., TPD or XPS data) specifically at 300 K to confirm that the oxygen has indeed depleted or migrated, rather than just relying on the theoretical model?

Authors reply: We did not perform a systematic investigation of the behaviour of O_{int} under different experimental conditions, since we concentrated our efforts on the experiments at 200 K, that gave more interesting results on ultrasmall Ni clusters. Nonetheless, clean MgO monolayers grown using the same protocol as the ones presented in the manuscript were monitored by XPS while cooling. As evident in figure R1, the overall O 1s signal is slightly larger at T<250 K than at RT, despite the Mg 1s signal remains unaltered.

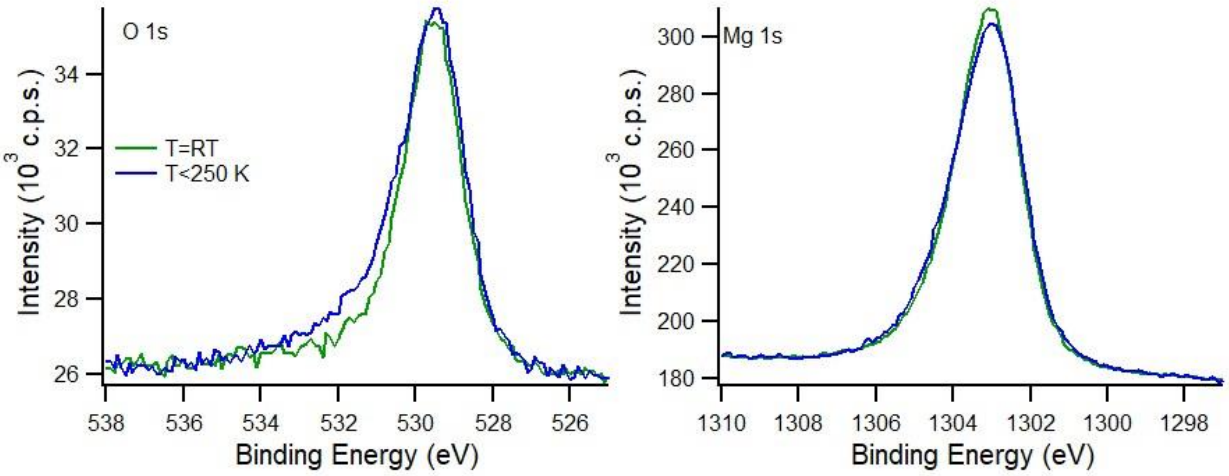


Figure R1. O 1s and Mg 1s spectra of 1 ML MgO/Ag(100) recorded at RT and while cooling the sample to liquid N2 temperature.

Although we agree that a more rigorous study would be necessary to provide a quantification of the amount of O_{int} at the different temperatures, e.g. discriminating it from possible water adsorption from the residual gas into the UHV chamber, we believe that these experimental data are coherent with the indications provided by DFT and free energy calculations.

9) Impact of Ni coverage on nucleation sites: While the spatial distribution is analyzed as a function of temperature, the manuscript does not detail how the total Ni coverage or deposition rate influences site selection. Would a higher Ni flux saturate the Oint trapping sites on the terraces faster, or would it lead to a different size distribution (e.g., larger clusters) that behaves differently regardless of the interfacial oxygen?

Authors reply: We thank the Reviewer for this interesting and appropriate question. We are sorry that, unfortunately, we cannot give a positive answer to it. Indeed, as stated also in the manuscript, our interest was primarily on ultra-small Ni clusters, corresponding to the first "magic numbers" or even smaller. For this reason, we always performed deposition of Ni atoms at low flux and remaining in the low coverage limit, in order to have the substrate temperature as the only variable. The need to limit the number of possible experiments was related to the fact that LT-STM measurements are time consuming. Each preparation has to be investigated for several days, up to 2-3 weeks, so that the experiments to be performed must be well defined and focussed. The choice of investigating small clusters vs substrate temperature was done considering the possibility to have a stronger theoretical support for clusters of limited size. We were now able to extend the analysis to larger aggregates, but not to further investigate the effect of the Ni coverage.

As a speculation, we expect that, if a significant increase of the Ni coverage leads to a larger number of clusters, at a given point the effect of O_{int} will be less relevant. Viceversa, if the effect of loading consists of an increase in the size, rather than in the number of clusters, then DFT calculations elucidate that even clusters above 1 nm size experience a stabilization in presence of interfacial oxygen. Thus, it is not easy to provide a conclusive answer to this question.

10) Role of other point defects: The study focuses on Oint as the primary stabilizing agent for terraces. Have the authors considered the role of other common oxide defects, such as F-centers (oxygen vacancies) or 0surface hydroxyls from residual vacuum water, which are known to act as nucleation sites on MgO? How can you be sure that Oint is the only significant factor in terrace stabilization?

Authors reply: The presence of O vacancies in a system bearing trapped O at the MgO/Ag interface is rather unlikely. The presence of surface OH is indeed a possibility, as correctly stated by the Referee. To rule out

this hypothesis under the experimental conditions presented in the manuscript, we rely both on literature and on some additional data that are reported in figure R2.

As demonstrated also by some of us, water adsorbs/dissociates at monolayer MgO/Ag(100) [L. savio et al., J. Phys. Chem. B 2004, 108, 7771]. In the cited paper, an evident OH peak is present around 3600-3700 cm^{-1} (approx. 450-460 meV) already after 1 L exposure both on the sample at RT and at low T. There is some general agreement that H_2O physisorbs on MgO terraces (https://doi.org/10.1016/S0039-6028(99)00730-X), while dissociation occurs at steps (https://doi.org/10.1557/jmr.2018.461).

In our experiment, water is never introduced into the UHV chamber so that H_2O adsorption/dissociation could come only from the rest vacuum as a contaminant, despite all efforts being done to minimize this unwanted effect.

According to the papers cited above, water from the rest vacuum should dissociate and OH should decorate the steps. If OH acts as anchoring point for Ni atoms, we should expect preferential nucleation at steps also at low T, when water contamination is expected to be higher, contrary to experimental evidence.

These speculations are supported by the analysis of HREEL spectra recorded during Ni clusters deposition at 200 K (Figure R2, previously published as Fig. 5 in ref. 33). They show no evident intensity in the OH-stretch region both before and after cluster growth, confirming that no significant water adsorption and/or dissociation has occurred from the rest vacuum during the time of the experiment.

Therefore, based on these spectra and on the previous literature, we rule out the possibility that adsorbed OH groups can act as nucleation centres of the Ni clusters in the experiments discussed in this manuscript and hence that they determine the spatial distribution of the latter ones.

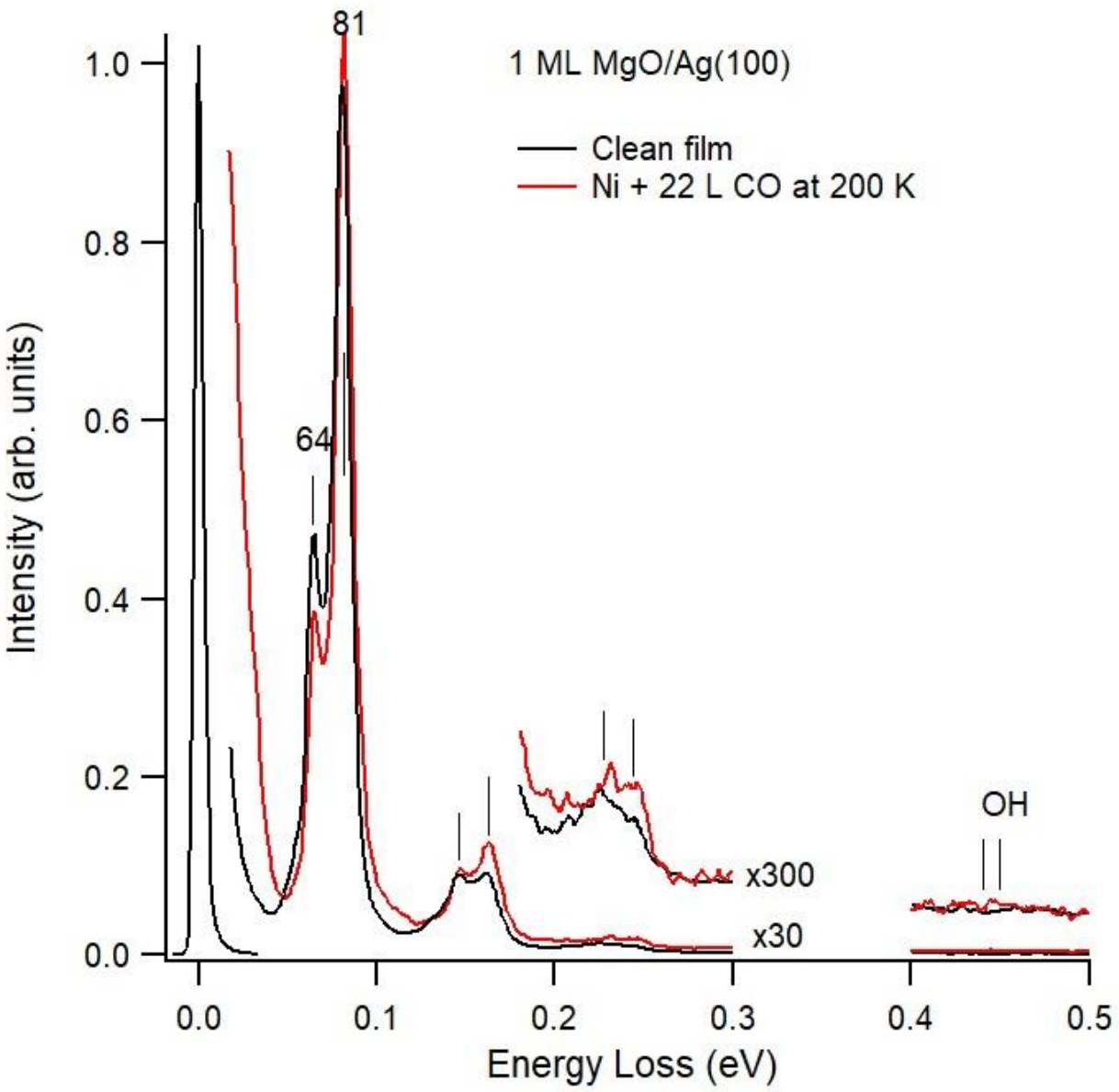


Figure R2. HREEL spectra of a 1 ML MgO/Ag(100) film equivalent to those discussed in the manuscript. The large losses at 64 and 81 meV and their replicas are due to the Fuchs Kliever modes typical of the monolayer oxide. Please note the magnification x300 of the OH-stretch region, that reveals absence of significant H_2O/OH coverage both before and after Ni clusters growth. Note that the additional exposure to CO performed in this experiment does not influence the outcome since CO does not adsorb on MgO under the present conditions. The low-intensity bands around 0.25 eV are due to overtones and combination bands of the fundamental MgO phonon modes.

We modified the text adding the following sentences on page 6:

We also remark that alternative explanations as the presence of F-centres or OH acting as nucleation centres at the terraces at low temperature can be excluded. On the one hand, oxygen vacancies are unlikely in presence of O_{int}; on the other hand, the presence of OH is excluded by vibrational spectroscopy analysis performed during CO exposure on Ni NC/MgO/Ag(100) [33].

11) Influence of epitaxial strain on cluster geometry: The DFT models assume icosahedral "magic number" clusters (Ni13, Ni55, Ni147) based on gas-phase stability. However, given the good lattice match between MgO and Ag(100), is it possible that epitaxial strain favors different isomers (like cuboctahedral or decahedral structures)? How would a change in the cluster's internal geometry affect the calculated adsorption energies and charge transfer results?

Authors reply: The choice of the "magic number" permits to adopt clusters of proven stability, displaying a metallic bulk and a 3D arrangement. The rationale of our choice relies as well on the possibility to consistently increase the size of the cluster, while maintaining its main structural and electronic properties. The cluster polymorphism is a very interesting topic, but it is indeed beyond feasibility. A caveat has been added at page 6:

"It must be stated, however, that other geometries could as well be possible, and an exhaustive study of the polymorphism in supported particles is beyond the scope of the present work. "

12) Cluster stability under reactive atmospheres: You conclude that the clusters are stable up to 600 K in UHV and are promising for CO2 methanation. However, catalytic reactions involve high partial pressures of H2 and CO2. How might the presence of these reactants influence the "reverse oxygen spillover" mechanism or the cluster's resistance to sintering compared to the UHV conditions reported here?

Authors reply: We agree with this remark, and we added a sentence at page 13:

"It must be stated, though, that the catalytic operating conditions do not envisage only high temperature, but also exposure to high pressure of reactive gases such as oxygen, hydrogen, CO_2 and others. Our previous computational work[34] assesses the stability of supported Ni clusters in an oxidizing environment, but their behaviour under reducing conditions and exposure to reactive gases remains to be investigated."

Reviewer #2: SURFIN-D-26-05175

The paper begins with an experimental observation from scanning tunneling microscopy (STM): Ni clusters on MgO/Ag(100) locate on flat terraces when grown at low temperature (T≤250K) but migrate to the step edges at room temperature. Supported by first-principles calculations, the authors attribute this behaviour to an oxygen spillover mechanism. Specifically, oxidized Ni clusters on flat terraces are stabilized by subsurface *oxygen dissolved in Ag but their energetics is lower at MgO edges when the system is in a metallic state. This work is a follow-up of Refs. 32-34 where similar observations were reported. Here, the authors propose a potential explanation for these findings.*

In my opinion, the reported phenomena are interesting and the paper is suitable for publication in Surfaces and Interfaces provided that the following points are clarified:

Authors reply: We are grateful for the thorough review of our manuscript and the substantially positive assessment of our work.

1) P6-first paragraph: The authors directly dismiss the hypothesis of diffusion-mediated accumulation of Ni clusters at step edges based solely on a few temperature data points, arguing that the transition is "too abrupt," and instead seek an alternative explanation based on subsurface oxygen. However, this argument is rather weak; homogenous nucleation (or heterogenous nucleation on MgO point defects?) may happen at low temperatures while heterogenous nucleation is more favoured at step edges at larger temperature. Furthermore, the "abruptness" argument could equally apply to their proposed interpretation involving subsurface oxygen. Why is the transition so abrupt? What is the actual underlying mechanism?

Authors reply: The reviewer raises a very relevant question. First of all, we agree that our claim on the abrupt nature of the transition observed from 250 K to 300 K should be mitigated, in light of the limited statistical sampling of growth temperatures and Ni loading (see also our answers to Reviewer 1). Moreover, the Reviewer is right in highlighting that the temperature will enhance the diffusion of Ni atoms, which might then meet and agglomerate at their thermodynamically most favoured surface site. However, the histogram in Figure 1 is not fully compatible with this simple picture. Indeed, if the aggregation at steps were to be considered as a bare thermal effect, one should observe a gradual change in distribution with temperature, and this is clearly not the case. One might then state that 300 K is a critical diffusion temperature for Ni adatoms, but such a hypothesis can be safely ruled out by the presence of large Ni aggregates at the surface even at 100 K. The clear turnover observed at 300 K, thus, requires a different explanation. In this paper, we present a possible explanation based on DFT calculations, which point at the specific role of the interfacial oxygen. We clarified this aspect by reformulating the text at page 6:

"Indeed, the relative population of NCs at step sites is between 20 and 30% for T≤250 K but it jumps to (89±3) % at 300 K (see Table S1 in Supporting Material)."

"Although diffusion certainly also plays a role in the present case, ~~the change in the relative population at steps and terraces is too abrupt to be explained only by this effect~~ the trend in relative population does not show any preferential nucleation at steps below 300 K, despite the fact that nanometric clusters do grow also at lower temperature"

2- *Aside Ni clusters, dark contrast features appear on the flat terraces of Fig. 1-a. Do they correspond to subsurface oxygen?*

Authors reply: Based on previous reports [https://doi.org/10.1021/acs.jpcc.8b12256, https://doi.org/10.1016/j.susc.2004.06.111], we tend to exclude that such features could be due to adsorbed water molecules, which should appear as bright spots. We cannot exclude, though, that these spots with lower contrast are actually due to non-uniform distribution of interfacial oxygen.{https://doi.org/10.1021/acs.jpcc.0c01248}

We added a sentence at page 6:

"Incidentally, dark spots are visible in Figs. 1a. An ultimate assignment on their nature cannot be provided, but we report that changes in contrast within MgO islands were previously attributed to non-uniform distribution of interfacial oxygen, affecting the local density of states of the MgO film.[31]"

3- Fig. 1: The cluster statistics is based on a limited number (x5) of 25x25 nm2 STM images. Given that the Ag surface may be rather heterogenous with step bunching, is it really relevant on a statistical point of view? Indeed, the overall surface topographies in Fig. 1 differ significantly between temperatures.

Authors reply: The surface topographies of Figure 1 present different terrace width and step density. These differences do not depend on the growth temperature of the Ni clusters but on the particular area imaged by STM. Indeed, in all cases the Ag(100) crystal was cleaned following the same sputtering and annealing procedure and the MgO monolayer was grown according to the protocol of ref. [28], also described in the experimental section.

However, the Reviewer is right in pointing out that the statistics is rather limited. Stimulated by their criticism, we revised our analysis including more images, that were initially left aside because of slightly lower resolution.

Now the new statistic extends over 10 images at 100 K, 13 images at 200 K, 5 images at 250 K and 11 images at 300 K. The outcome of the new analysis, reported in the revised version of Figure 1e) and in the new Table S1 of the Supporting Material, further supports our interpretation of the data since the population of Ni NCs at steps remains almost stable around for T≤250 K and increases suddenly to (89±3) % at RT.

The caption of Figure 1e) and the text on page 6 were updated with the new statistics information. In addition, the following sentence was added in the discussion on page 6:

"The overviews in Figure a)-c) may appear different, but this is mainly due to the different step density of the imaged MgO areas since statistical analysis over several images (Figure 1e) indicates a similar population of Ni NCs at steps for T≤250 K. Vice versa, the outcome at 300 K suggests the activation of a different mechanism."

4- *The fate of O at 300K is not discussed either theoretically or experimentally, yet it is central to the interpretation. The authors favour a temperature-induced diffusion into the large Ni clusters over a dissolution in the Ag bulk. Would it be possible to derive the activation barrier if oxygen diffusion occurs via an atom exchange through the MgO? Are there any signatures of changes in Ni cluster chemistry, e.g., in XPS core levels between low temperature and 300K? An alternative explanation could involve growth dynamics, with more mobile O-Ni entities (such as the reported oxidized NixOy clusters, where x = 4-6).*

Authors reply: We tried to calculate the energy barrier related to O diffusion via replacement of lattice MgO, but the non-trivial reaction path, involving many atoms, makes the task quite difficult. In a previous computational report (ref. 34), we did not observe reverse spillover phenomena taking place during AIMD runs at 200 K. This does not provide an ultimate reply, though. It is also useful to recall the ab initio thermodynamics data reported in Table S2, which shows that the interfacial oxygen depletion could take place at temperatures between 300 and 400 K (based on DFT binding energies), starting from step regions, where O_{int} is bound less strongly.

A relevant experimental hint is provided by the XPS measurements on clean MgO reported in Fig. R1 (please see our replies to Reviewer 1, point 8), which seems to indicate the O_{int} evaporation at RT is possible. The consideration of the Reviewer on the diffusion of Ni-O entities is also definitely true.

We added a few sentences at page 12 to summarize all these elements:

"It is also interesting, in this respect, to mention that the different O_{int} stability in ML_c and BL_c (i.e. in the central region of MgO islands) compared to steps could induce oxygen diffusion within the MgO/Ag interface. Overall, the ~~The~~ O_{int} concentration can vary due to various factors; […]"

"It implies a concerted mechanism in which O atoms from the MgO lattice move to the Ni cluster borders and the oxygen vacancies are refilled by interfacial oxygen species.[34] It was not possible, though, to evaluate the actual diffusion barrier for this process."

"The diffusion of partially oxidized Ni_xO_y entities could, in principle, also contribute to further non-trivial growth mechanisms. "

5- I suggest introducing the final interpretation of the paper immediately after the description of the STM images (P6), rather than waiting until the end of the paper (P12). This would help readers unfamiliar with the topic to follow the reasoning more easily

Authors reply: We agree with this remark, and we therefore added a paragraph at page 6 anticipating the outline of the forthcoming discussion:

"As it will be discussed in the following, our findings envisage that the presence of interfacial oxygen between MgO and Ag could enhance the clusters stability on terraces. The limited thermal stability of O_{int}, though, may explain the preferential growth at steps at 300 K. "

6- Last sentence of P10 ("The different effect….Ag support") is really unclear.

Authors reply: The Reviewer is right. This sentence has been rephrased as follows:

"The different effect of an analogous concentration of interfacial oxygen on MgO MLs and BLs can be attributed to the different thickness of the insulating MgO layers. As expected, the effect of O_{int} is smaller on thicker BLs compared to MLs.~~ultimate thickness limit of the insulating MgO layer separating the adsorbed Ni clusters from the Ag support.~~ "

7- The assertion P11 "Indeed, the uniform distribution… considered here" is clearly overstated. This does not constitute proof. Moreover, no Ni cluster size distribution is provided in the paper.

Tentative reply: In compliance with this remark, we softened the statement at pages 11-12:

"Indeed, ~~the uniform distribution of clusters observed experimentally at 100 K suggests that Ni adatoms have enough kinetic energy to diffuse on the surface at any temperature considered here~~ the presence of aggregations larger than few-atoms aggregates at 100 K already, in agreements with previous report [33], is a key-point in indicating the presence of a mechanism acting beyond bare thermally enhanced diffusion"